buildings

MDPI

Article

Correlation Analysis and Dynamic Evolution Research on Safety Risks of TBM Construction in Hydraulic Tunnels

Xiangtian Nie [1], Hui Yu [1], Jilan Lu [2], Peisheng Zhang [1] and Tianyu Fan [1,*]

[1] School of Water Conservancy, North China University of Water Resources and Electric Power, Zhengzhou 450046, China; niexiangtian@ncwu.edu.cn (X.N.)
[2] Shanghai General Station of Immigration Inspection, Shanghai 200120, China
* Correspondence: fantianyu@ncwu.edu.cn

Abstract

To enhance the safety risk management and control capabilities for TBM (Tunnel Boring Machine) construction in hydraulic tunnels, this study conducts a correlation analysis and dynamic evolution study of safety risks. Data were collected through multiple channels, including a literature review, on-site records, and expert interviews. Grounded theory was employed for three-level coding to initially identify risk factors, and gray relational analysis was used for indicator optimization, ultimately establishing a safety risk system comprising 5 categories and 21 indicators. A multi-level hierarchical structure of risk correlation was established using fuzzy DEMATEL and ISM, which was then mapped into a Bayesian network (BN). The degree of correlation was quantified based on probabilistic information, leading to the construction of a risk correlation analysis model based on fuzzy DEMATEL–ISM–BN. Furthermore, considering the risk correlations, a safety risk evolution model for TBM construction in hydraulic tunnels was developed based on system dynamics. The validity of the model was verified using the AY project as a case study. The results indicate that the safety risk correlation structure for TBM construction in hydraulic tunnels consists of 7 levels, with the closest correlation found between "inadequate management systems" and "failure to implement safety training and technical disclosure". As the number of interacting risk factors increases, the trend of risk level evolution also rises, with the interrelations within the management subsystem being the key targets for prevention and control. The most sensitive factors within each subsystem were further identified as adverse geological conditions, improper construction parameter settings, inappropriate equipment selection and configuration, weak safety awareness, and inadequate management systems. The control measures proposed based on these findings can provide a basis for project risk prevention and control. The main limitations of this study are that some probability parameters rely on expert experience, which could be optimized in the future by incorporating more actual monitoring data. Additionally, the applicability of the established model under extreme geological conditions requires further verification.

Keywords: hydraulic tunnel; TBM; risk evolution; risk correlation; system dynamics

check for updates

Academic Editors: Bingxiang Yuan, Waseim Ragab Azzam, Binbin Yang and Shiyuan Huang

Received: 24 July 2025
Revised: 1 September 2025
Accepted: 4 September 2025
Published: 17 September 2025

Citation: Nie, X.; Yu, H.; Lu, J.; Zhang, P.; Fan, T. Correlation Analysis and Dynamic Evolution Research on Safety Risks of TBM Construction in Hydraulic Tunnels. *Buildings* **2025**, *15*, 3359. https://doi.org/10.3390/buildings15183359

Copyright: © 2025 by the authors. Licensee MDPI, Basel, Switzerland. This article is an open access article distributed under the terms and conditions of the Creative Commons Attribution (CC BY) license (https://creativecommons.org/licenses/by/4.0/).

1. Introduction

Hydraulic tunnels are an essential component of modern water conservancy engineering systems, playing a key role in inter-regional water resource allocation, clean energy development, and flood control and drainage. The application of full-face Tunnel Boring

Machine (TBM) technology can significantly improve the efficiency and quality of tunnel construction. However, as TBM construction for hydraulic tunnels is a form of underground engineering, the risk factors affecting construction safety are characterized by concealment, multiplicity, and strong correlations. Actual engineering cases have fully demonstrated its high-risk nature. For example, during the Lanzhou water source construction project, a TBM became stuck in a granite formation due to shield compression from uneven stress. In the Northwest Qionghai Water Supply Project, fissure water infiltration weakened the mechanical properties of the rock mass, inducing instability at the tunnel face. The project to divert the Datong River to the Huangshui River encountered large deformation of the surrounding rock and support failure in a high-stress fault zone, leading to severe deviation of the TBM's alignment and a halt in construction. These complex correlations cause risk levels to change continuously over time, seriously threatening the reliability of project construction. Therefore, conducting research on the correlation analysis and evolution of safety risks in TBM construction for hydraulic tunnels is of great significance for ensuring safety and stability during the construction process and enhancing the reliability of the TBM system.

In recent years, both domestic and international scholars have conducted research on the construction safety of hydraulic tunnels and TBM projects. Zhang et al. [1] developed a comprehensive TBM safety risk evaluation model by introducing multi-level intersecting membership functions based on fuzzy normal distribution. Hu et al. [2] proposed a deep drainage tunnel risk assessment framework integrating ISM, CRITIC, and the cloud model, which enhanced assessment accuracy through structural modeling and objective weighting. Sharafat et al. [3] employed a bow-tie approach combining fault and event trees to quantify the coupled effects of geological uncertainty and human errors, highlighting the significance of multi-risk interactions. Chung [4] compared three TBM tunneling risk models and introduced a causal-network-based risk matrix with a modified weighting scheme, demonstrating improved reliability and robustness. Hasanpour et al. [5] combined artificial neural networks and Bayesian networks to predict TBM jamming risks under adverse geological conditions, establishing a thrust-estimation model effective even with incomplete geological data. Wang Jie et al. [6] integrated grounded theory, hybrid weighting (AHP–entropy–game theory), and the cloud model to construct a risk evaluation system for long-distance, small-diameter tunnels, improving risk identification accuracy. Liu Wanlin et al. [7] advanced an improved G2-AEW-UMT model with barrier factor diagnosis to identify key risk sources, quantitatively assessing the impacts of climatic, hydrological, and geological conditions in the Central Yunnan Water Diversion Project. Wang Junwu et al. [8] applied the HAZOP method, combined with rough set theory and the cloud model, to evaluate shield tunneling risks in deep drainage tunnels, identifying high-risk factors such as delayed parameter adjustment and insufficient training. Li Qiang et al. [9] constructed a WBS-RBS-based risk matrix for water diversion tunnels, determining factor weights via analytic hierarchy process and formulating targeted control measures to strengthen safety management.

In practical projects, risk factors are not only interrelated but also exhibit dynamic variability, which has motivated a number of studies on risk correlation and evolution. Regarding risk correlation, Fu et al. [10] combined association rule mining with weighted network theory to construct a risk correlation analysis framework for deep foundation pit projects, enabling the analysis of complex interdependent risk factors. Yan et al. [11] applied the N-K model to evaluate risk associations, quantifying the probabilities and magnitudes of different risk combinations, and thereby providing a novel quantitative framework. Li et al. [12], building on the DEMATEL–ISM method, employed Bayesian networks to quantify causal interactions among accident-inducing factors, and verified the

model's ability to deliver clear and actionable risk information for safety management. Nie Xiangtian et al. [13] integrated DEMATEL–ISM, risk entropy, and accident risk transmission theory to develop a correlation and transmission model for long-distance water diversion projects, offering a scientific basis for risk management in similar engineering contexts. Wu Yajun et al. [14] analyzed interdependencies among risk events in artificial ground-freezing construction and established a fuzzy comprehensive evaluation model based on correlation degree and probability, thereby addressing the limitations of conventional methods that neglect risk interdependence and providing a quantitative basis for targeted risk control strategies. In terms of risk evolution, Huang et al. [15] employed complex network theory to construct a network-based model of construction risk correlations, advancing theoretical research on the evolutionary mechanisms of risk coupling. Wu Caodong et al. [16] combined N-K model coupling degree calculations with system dynamics to simulate risk evolution trends under interdependent conditions, providing a scientific foundation for targeted risk control. Xie Luqiang et al. [17] overcame the limitations of traditional independent risk analysis by developing an integrated approach to correlation modeling and quantitative evaluation, offering a more systematic and dynamic paradigm for risk studies in TBM hydraulic tunnel projects, particularly under complex geological conditions involving multi-risk coupling.

Building on these contributions, the present study seeks to integrate the strengths of existing methods with the unique risk characteristics of TBM hydraulic tunnel construction. Specifically, it aims to develop a comprehensive model capable of simultaneously analyzing the intricate correlation structures among risk factors and simulating their dynamic evolution. This approach is intended to address the current research gap in systematic and dynamic risk analysis, and to provide a quantitative decision-making basis for safety risk management in TBM hydraulic tunnel construction.

2. Safety Risk Index System for TBM Construction of Hydraulic Tunnel

2.1. Data Collection

To address the specific characteristics of hydraulic tunnel TBM construction, this study collected a substantial body of textual data, including literature sources, construction risk event reports, and interview records.

(1) Literature sources

Literature sources, as systematically studied and academically validated information, provide theoretical support and empirical reference for this research. With construction safety as the primary focus, the selection of risk factors for hydraulic tunnel TBM construction was informed by domestic and international studies. The databases China National Knowledge Infrastructure (CNKI) and Web of Science were used for data retrieval. For Chinese literature, journal sources were restricted to EI, CSSCI, and CSCD, while both Chinese and English high-quality journal papers, as well as master's and doctoral dissertations, were included. Search topics and keywords consisted of "Tunnel construction", "Safety risks in the construction of hydraulic tunnels", "TBM construction", and "Safety risks of TBM construction in hydraulic tunnels".

(2) Case reports

Both online and offline approaches were adopted to collect case reports of TBM construction risk events in hydraulic tunnels that occurred in recent years in China. Online data were obtained from official databases and government portals, including the Ministry of Emergency Management of the People's Republic of China, as well as provincial, municipal, and district emergency management departments. Field investigations were also conducted to complement the database records.

(3) Interview records
The AY hydraulic tunnel project was selected as the primary subject for interviews. Participants included project managers, engineers, and frontline workers who had either full-cycle experience with TBM construction or direct involvement in handling major TBM risk events. The interviews focused on sources of risk, mechanisms of hazard formation, response measures, and subjective perceptions of TBM construction safety. The collected interview materials were standardized by consolidating similar content and eliminating colloquial expressions, resulting in structured transcripts suitable for subsequent analysis.

2.2. Grounded Theory Workflow

2.2.1. Open Coding

The analysis was conducted around core terms such as "adverse impact", "problem", "risk", and "safety". In the literature review, particular attention was paid to the risk indicator systems identified by different scholars, while the case reports were examined in light of accident causation theory. By systematically mining textual data related to safety risk descriptions, event characteristics, construction behaviors, and contextual factors, a set of basic conceptual units was developed. Through multiple rounds of refinement, redundant and repetitive information was removed, and the textual content was abstracted into conceptual codes. Using Nvivo14 software, which facilitates the identification of intrinsic connections among data, corresponding nodes were established. The conceptualized texts were further iteratively screened, repeatedly integrating discrete concepts to build a more hierarchical coding framework. Ultimately, a number of inductive initial categories were derived. Although these categories directly corresponded to safety risks in hydraulic tunnel TBM construction, they remained relatively fragmented and therefore required further refinement and integration.

2.2.2. Axial Coding

Axial coding was then applied to integrate the initial categories obtained during open coding. By analyzing the underlying meanings of the data, more concise core categories were constructed through clustering. This process not only addressed the limitations of open coding—where the initial categories tend to be isolated and scattered—but also established logical linkages among different core categories, thereby laying the foundation for selective coding. Due to space limitations, partial examples of the axial coding is shown in Table 1.

Table 1. Partial examples of axial coding.

Main Categories	Initial Category
Advance geological prediction problem	Inaccurate or unrealistic geological forecasts; Substandard exploration quality; lag in advance geological prediction; lack of geological monitoring
Improper construction parameter setting	Inappropriate cutterhead speed, torque, or thrust; Incorrect excavation speed; improper settings for gripper shoes or grouting parameters
TBM attitude deviation	Deviation in TBM excavation path; improper axis control; difficulty in TBM attitude control
Poor support effect	Deformation of support structures; insufficient support strength; leakage in permanent lining; untimely or substandard support installation; inadequate synchronous grouting; omission of secondary grouting; grout leakage; lag in backfilling procedures; improper grouting control
Improper slag control	Discontinuous muck removal; excessive muck volume; low muck removal rate; risks associated with conveyor belt operation; improper muck handling operations

Table 1. *Cont.*

Main Categories	Initial Category
Improper equipment maintenance	Lack of regular inspection and maintenance; incorrect maintenance procedures; use of poor-quality or mismatched spare parts
Bad geological condition	Weak interlayers or faults; fracture zones; significant variations in lithology; extremely soft rock formations; shallow burial sections
Adverse hydrological conditions	High groundwater concentration; excessively high groundwater table; corrosive groundwater; high groundwater head pressure
Insufficient technical level	Lack of operator proficiency; inadequate technical skills; insufficient construction experience; low level of workmanship
Poor physical and mental condition	Negative work attitude; lack of concentration; weak safety awareness
Violation of regulations	Non-compliance with construction procedures; rushing the construction schedule; unauthorized operations; improper command or direction
Unreasonable staffing	Unqualified personnel; vacant positions; poor utilization of human resources

2.2.3. Selective Coding

Selective coding was conducted by classifying the major categories according to their intrinsic logical relationships and essential attributes. For example, categories such as improper muck removal control and TBM excavation conditions were both attributable to inappropriate construction operations, and thus were grouped under the core category of technical risk. Similarly, from the perspective of the subjects generating safety hazards, factors such as work proficiency and working status, which are constrained by individual subjectivity, were categorized as personnel risk. Following the same analytical logic, other major categories were systematically examined, leading to the identification of five sub-core categories. Since this study focuses on safety risks in hydraulic tunnel TBM construction, these were consolidated into the core categories of the grounded theory framework.

To test the scientific validity and completeness of the risk categories identified through grounded theory, a theoretical saturation test was conducted using the Delphi method in combination with textual data validation. Specifically, a panel of ten experts—including researchers and academics specializing in hydraulic structures, construction safety management, and risk management, as well as frontline technical staff with practical TBM construction experience—was invited to review the categories derived from the grounded theory analysis and provide guidance and recommendations. The partial information of experts in the expert group is presented in Table 2.

Table 2. Partial information of experts in the expert group.

Serial Number	Workplace	Research Direction	Professional Title	Years of Experience
1	Scientific Research Institute	Intelligent Construction for TBM Tunneling	Researcher	22
2	Hydraulic Engineering Construction Company	Application of TBM Key Technologies	Senior Engineer	25
3		TBM Construction Management	Engineer	20
4	Higher Education Institution	Construction Management of Hydraulic Structures	Professor	30
5		Risk Management in Hydraulic Engineering	Associate Professor	24

2.3. Gray Relational Analysis

Gray relational analysis (GRA) was employed to rank and select the initially identified risk factors according to their importance. A total of 20 experts were invited to evaluate each factor on a scale of 1–10 from two dimensions: the likelihood of occurrence and the degree of impact. The maximum score of each factor was used to construct the reference sequence, while the expert ratings were treated as the comparative sequences. After normalization and dimensionless processing by the mean method, the gray relational coefficients and the relational degree were calculated. The formula for calculating the relational degree is given in Formula (1).

$$r_i = \frac{1}{n}\sum^{n}\xi_i(k) \quad (1)$$

Factors with a gray relational degree not lower than 0.6 were retained. For geological risks, the selected factors included adverse geological conditions, unfavorable hydrogeological conditions, surrounding rock deformation and instability, and sudden mud inrush or water gushing. Following the same computational procedure, the gray relational degrees of all safety risk factors associated with hydraulic tunnel TBM construction were obtained. Through this process, the final safety risk indicator system for hydraulic tunnel TBM construction was established, as presented in Table 3.

Table 3. Safety risk indicator system for hydraulic tunnel TBM construction.

	Level One Risk	Level Two Risk	Number
Safety Risk of TBM Construction in Hydraulic Tunnel	Geological risk X_1	Bad geological condition	X_{11}
		Adverse hydrological conditions	X_{12}
		Deformation instability of surrounding rock	X_{13}
		Mud outburst and water gushing	X_{14}
	Technical risk X_2	Advance geological prediction problem	X_{21}
		Improper construction parameter setting	X_{22}
		TBM attitude deviation	X_{23}
		Poor support effect	X_{24}
		Improper slag control	X_{25}
	Equipment risk X_3	Improper equipment selection and configuration	X_{31}
		Shield, cutterhead blocked	X_{32}
		Main bearing or seal failure	X_{33}
		Cutter head wear damage	X_{34}
		Improper equipment maintenance	X_{35}
	Personnel risk X_4	Insufficient technical level	X_{41}
		Weak safety awareness	X_{42}
		Violation of regulations	X_{43}
	Management risk X_5	Management system insufficiency	X_{51}
		Safety training and technical briefing implementation deficiency	X_{52}
		Site safety control deficiency.	X_{53}
		Unreasonable staffing	X_{54}

The division of the five risk subsystems was established based on the systemic characteristics of hydraulic tunnel TBM construction and the multidimensional nature of risk sources. Geological risk represents external environmental factors; technical risk reflects the level of operation and control during the construction process; equipment risk concerns the reliability of mechanical systems; personnel risk highlights the critical role of human factors; and management risk addresses overall coordination from an organizational perspective. This framework not only encompasses the full spectrum of risk sources throughout the construction process but also aligns with the management logic of systems

engineering, thereby providing a clear basis for subsequent analyses of risk correlation and dynamic evolution.

3. Safety Risk Correlation Analysis of Hydraulic Tunnel TBM Construction Based on Fuzzy DEMATEL–ISM–BN Method

3.1. Fuzzy DEMATEL–ISM–BN Method

The DEMATEL method constructs a comprehensive influence matrix that reflects the logical relationships and intrinsic characteristics among factors, enabling micro-level analysis of the attributes, importance, and causal relationships of various risk factors. However, it cannot directly determine the hierarchical structure of factors. To overcome this limitation, the ISM method was integrated into this study. By setting thresholds and decomposing the reachability matrix, ISM provides a macro-level hierarchical interpretation of the influence mechanisms among factors. This process generates a multi-level hierarchical model that distinguishes direct, indirect, and fundamental factors, thereby achieving both hierarchical classification and correlation analysis of risk factors. The combination of DEMATEL and ISM not only complements the analysis of inter-factor relationships but also simplifies the matrix computation process of ISM by transforming the comprehensive influence matrix generated by DEMATEL into a reachability matrix.

In addition, to minimize subjectivity in expert evaluations, fuzzy set theory was introduced by applying triangular fuzzy numbers (TFNs) to process expert scoring data [18,19]. A TFN is defined by three parameters—minimum value, most likely value, and maximum value—which together describe the fuzziness of the object under study. Formally, in the real number domain, a fuzzy number with membership function $F(x)$ is called a triangular fuzzy number if it satisfies the condition expressed in Formula (2).

$$F(x) = \begin{cases} 0, & x < l \\ \frac{x-l}{m-l}, & l < x \leq m \\ \frac{r-x}{r-m}, & m < x \leq r \\ 0 & x > r \end{cases} \tag{2}$$

In the equation, r represents the upper bound of fuzziness, l represents the lower bound, and m denotes the most likely value corresponding to the peak of the membership function. A triangular fuzzy number is denoted as (l, m, r), where $l \leq m \leq r$. The Triangular fuzzy number affiliation diagram is illustrated in Figure 1.

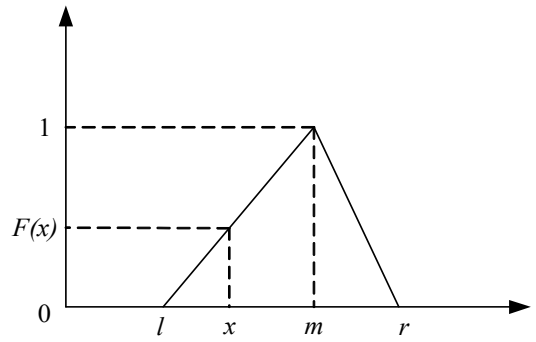


Figure 1. Triangular fuzzy number affiliation diagram.

However, the fuzzy DEMATEL–ISM model still has limitations in quantitative analysis, as it cannot precisely measure the strength of influence among factors. To overcome this, the hierarchical structure generated by ISM was mapped onto the topology of a Bayesian network (BN). Probability parameters were then estimated by incorporating TFNs together

with the Noisy-or gate model. Leveraging the inference capability of BN, probabilistic distributions were used to quantify the strength of associations among risk factors, thus enabling an accurate characterization and dynamic reasoning of risk correlations.

This integrated approach balances qualitative analysis with quantitative evaluation, progressing from factor correlation identification to hierarchical structure construction, and further to probabilistic association measurement. In doing so, it establishes a systematic methodological framework for risk analysis.

3.2. Flow Chart of Safety Risk Correlation Analysis for Hydraulic Tunnel TBM Construction

For the safety risk factors in the TBM construction process of hydraulic tunnels, the DEMATEL method is utilized, integrating expert knowledge. A comprehensive influence matrix is established based on triangular fuzzy numbers to calculate the influence degree, affected degree, centrality and cause degree, and analyze the causal attributes and importance distribution of the factors [20]. Secondly, the ISM method is applied to convert the comprehensive influence matrix into a standard reachability matrix, and a multi-level hierarchical risk correlation structure model is constructed to clarify and structure the complex factor relationships and reveal the interaction paths among various risk factors [21–23]; Map the risk association structure to the BN topological structure and, with the help of the reasoning function of the BN model, represent the association degree between nodes in terms of probability distribution information [24]. The flowchart of Safety Risk Correlation Analysis for Hydraulic Tunnel TBM Construction is illustrated in Figure 2.

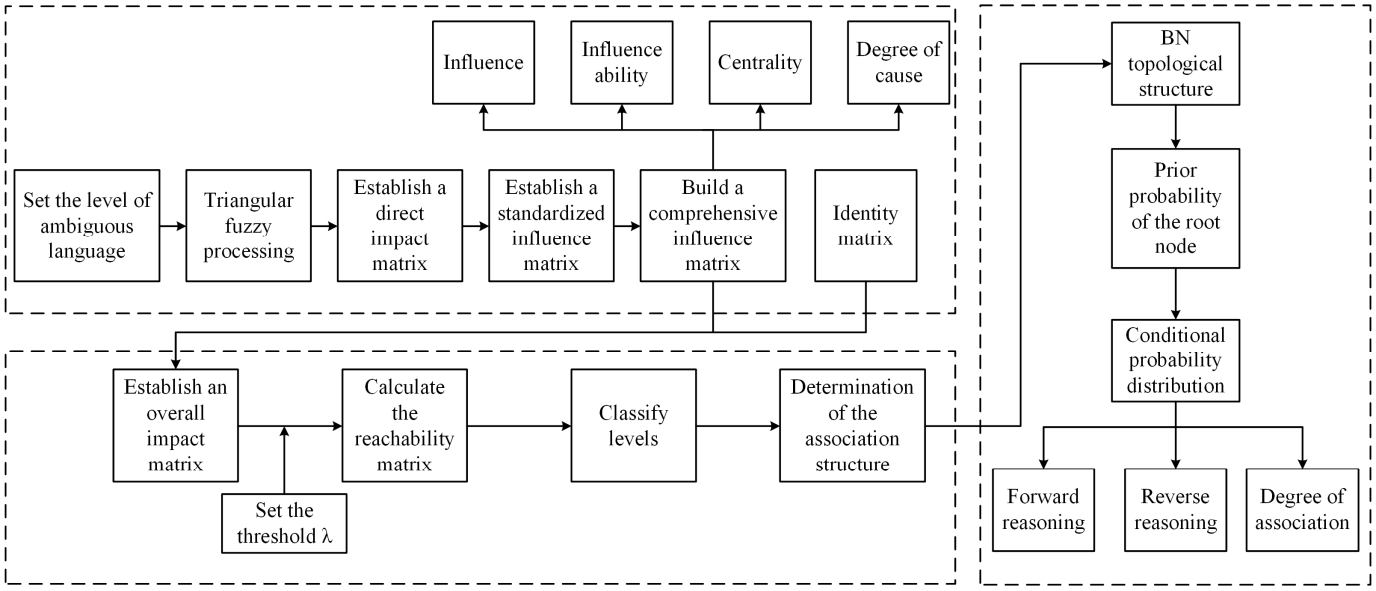


Figure 2. Flowchart of safety risk correlation analysis for hydraulic tunnel TBM construction.

3.3. Construction of Fuzzy DEMATAL–ISM–BN Model

1. Construct the direct impact matrix *B*. In the traditional DEMATEL method, expert scoring is used to evaluate the degree of mutual influence among factors. To effectively address the linguistic fuzziness and subjective uncertainty inherent in such expert judgments, this study improved the conventional DEMATEL method by incorporating fuzzy set theory.

   To ensure the convergence and reliability of expert group judgments, a multi-round anonymous consultation process based on the Modified Delphi Method was adopted. The specific steps are as follows:

   Step 1: Expert group formation and preparation.

   Ten experts with substantial theoretical knowledge and practical experience in hy-

draulic tunnel TBM construction, safety management, and risk analysis were carefully selected. Their backgrounds covered research institutes, universities, and frontline engineering organizations, ensuring diverse perspectives (see Table 2). Before the consultation, each expert was provided with standardized background materials, including detailed definitions of 21 risk factors, an overview of the AY project, and explicit scoring criteria (e.g., the semantic scale of triangular fuzzy numbers shown in Table 4). This preparation ensured a consistent understanding of the evaluation objects and standards.

Table 4. Semantic transformation grade table of triangular fuzzy numbers.

Rating Description	Triangular Fuzzy Number
No influence—NO	(0.0, 0.1, 0.3)
Weak influence—VL	(0.1, 0.3, 0.5)
Minimal influence—L	(0.3, 0.5, 0.7)
Moderate influence—H	(0.5, 0.7, 0.9)
Significant influence—VH	(0.7, 0.9, 1.0)

Step 2: Independent initial anonymous scoring (Round 1).
Each expert independently and anonymously evaluated the influence relationships among all pairs of risk factors without interference from others. Triangular fuzzy numbers were applied to capture not only the degree of influence but also the uncertainty embedded in expert judgments. The anonymity and independence of this round aimed to eliminate authority bias or groupthink effects on the initial evaluations.
Step 3: Statistical analysis and anonymous feedback (Round 2).
After collecting the first-round scores, the research coordinators conducted statistical analysis of the triangular fuzzy numbers for each evaluation, calculating measures such as mean, median, and dispersion indices (e.g., standard deviation or interquartile range). An anonymous feedback report was then distributed to all experts. This report included: (1) a statistical summary of group evaluations for each item; (2) the individual expert's own previous score; and (3) for items with high dispersion, anonymous justifications provided by experts who had given extreme ratings (highest and lowest).
Step 4: Iterative revision and consensus building.
After reviewing the feedback report, experts reconsidered and refined their initial judgments in light of the group consensus and the reasoning of others. They could either maintain their original scores with additional justification or adjust their ratings toward group consensus. This iterative process was repeated until the dispersion of expert opinions for all evaluation items (measured, for example, by the coefficient of variation) fell below the predefined threshold of 0.15, and the mean ratings stabilized across two consecutive rounds. This indicated that an acceptable level of consensus had been achieved. Through this rigorous iterative process, the final aggregated evaluation values were obtained and used to construct the initial direct influence matrix B, thereby enhancing the objectivity of the data and the robustness of the study's conclusions.
The evaluation grades of experts are transformed into triangular fuzzy numbers, and $(l_{ij}^k, m_{ij}^k, r_{ij}^k)$ is used to express the scoring result of the influence degree of the i-th factor on the j-th factor in the factor set by the k-th expert, where $k \in \{k|1, 2, \ldots, n\}$. The CFCS method is applied to defuzzification.

(1) Normalization processing of triangular fuzzy numbers. For the structural form of triangular fuzzy numbers, the process is shown in Formulae (3)–(5):

$$x_{lij}^{k} = \frac{l_{ij}^{k} - \min l_{ij}^{k}}{\max r_{ij}^{k} - \min l_{ij}^{k}} \tag{3}$$

$$x_{mij}^{k} = \frac{m_{ij}^{k} - \min m_{ij}^{k}}{\max r_{ij}^{k} - \min l_{ij}^{k}} \tag{4}$$

$$x_{rij}^{k} = \frac{r_{ij}^{k} - \min l_{ij}^{k}}{\max r_{ij}^{k} - \min l_{ij}^{k}} \tag{5}$$

(2) Calculate the standard value of triangular fuzzy number. After converting the normalized triangular fuzzy number to the left standard value x_{lij}^{*k} and the right standard value x_{rij}^{*k}, calculate the total standard value x_{ij}^{k}, as shown in Formulae (6)–(8):

$$x_{lij}^{*k} = \frac{x_{mij}^{k}}{1 + x_{mij}^{k} - x_{lij}^{k}} \tag{6}$$

$$x_{rij}^{*k} = \frac{x_{rij}^{k}}{1 + x_{rij}^{k} - x_{mij}^{k}} \tag{7}$$

$$x_{ij}^{k} = \frac{x_{lij}^{*k}(1 - x_{lij}^{*k}) + x_{rij}^{*k} x_{rij}^{*k}}{1 - x_{lij}^{*k} + x_{rij}^{*k}} \tag{8}$$

(3) Defuzzification. The score result of the k-th expert regarding the influence degree of the i-th factor on the j-th factor is calculated and converted to the clear value b_{ij}^{k}, as shown in Formula (9):

$$b_{ij}^{k} = \min l_{ij}^{k} + x_{ij}^{k} \times (\max r_{ij}^{k} - \min l_{ij}^{k}) \tag{9}$$

According to the above steps, after the fuzzy scores of all experts on the influence degree of the i-th factor on the j-th factor are converted to clear scores, the average value b_{ij} of the scores of the i-th factor on the j-th factor is calculated by using Formula (10). The influence values among the factors after defuzzification are filled into the matrix to construct the direct influence matrix B, as shown in Formula (11).

$$b_{ij} = \frac{1}{n} \sum_{k=1}^{n} b_{ij}^{k} \tag{10}$$

$$B = \left[b_{ij} \right]_{n \times n} \tag{11}$$

2. Establish a normalized influence matrix *G*. Normalize the direct influence matrix *B* by using the row sum maximum normalization method to obtain a normalized direct influence matrix G, as shown in Formula (12).

$$G = \frac{1}{\max\limits_{1 \le i \le n} \sum\limits_{j}^{n} b_{ij}} B \tag{12}$$

3. Calculate the comprehensive influence matrix D. The comprehensive influence matrix represents the direct influence and indirect influence relationship between all factors, and the calculation process is shown in Formula (13).

$$D = (G + G^2 + \ldots + G^n) = \sum_{n=1}^{\infty} G^n = G(I - G)^{-1} \tag{13}$$

where I is the identity matrix.

4. Based on the comprehensive influence matrix D, the influence degree (e_i), affected degree (f_i), centrality (M_i), and causality (N_i) of each factor can be calculated. The influence degree e_i represents the total impact of a single factor on all other risk factors. A larger value indicates that the factor has a stronger driving force on the overall system. The calculation formula is expressed as follows:

$$e_i = \sum_{j=1}^{n} d_{ij} \ (i = 1, 2, \ldots, n) \tag{14}$$

5. The affected degree (f_i) represents the total influence that an individual factor receives from all other risk factors. A larger value indicates that the factor is more susceptible to the influence of other factors. The calculation formula is expressed as follows:

$$f_i = \sum_{j=1}^{n} d_{ij} \ (i = 1, 2, \ldots, n) \tag{15}$$

6. The centrality (M_i) represents the overall importance of an individual factor within the entire complex system. It is obtained as the sum of its influence degree and affected degree. A larger value of M_i indicates that the factor has a greater impact on the overall changes in the system. The calculation formula is expressed as follows:

$$M_i = e_i + f_i \tag{16}$$

7. The causality (N_i) represents the tendency of an individual factor in terms of its influencing attributes. It is obtained as the difference between its influence degree and affected degree. A larger value of N_i indicates that the factor is more likely to act as a driving element within system changes. If $N_i > 0$, factor i is classified as a cause factor; otherwise, it is regarded as an effect factor. The calculation formula is expressed as follows:

$$N_i = e_i - f_i \tag{17}$$

8. Generate the reachable matrix K. Combine the comprehensive influence matrix D with the identity matrix I to establish the overall influence matrix O, and consider that the influence degree between some factors is small, introduce a threshold λ to optimize the matrix O, λ is the sum of the matrix of the comprehensive influence matrix D and the standard deviation. Use the Formula (19) to transform the elements in the matrix to obtain the reachable matrix K. The calculation formulas are as follows:

$$O = \left[o_{ij}\right]_{n \times n} = I + D \tag{18}$$

$$k_{ij} = \begin{cases} 1, & o_{ij} \geq \lambda \\ 0, & o_{ij} < \lambda \end{cases} \tag{19}$$

9. Divide factor hierarchy. Reachability set L_i consists of factors corresponding to columns with median 1 in each row of reachability matrix K; antecedent set Q_i consists of factors corresponding to rows with median 1 in each column of reachability matrix K. If there is a certain factor h_i satisfying Formula (20), it indicates that h_i is the highest level factor, and then delete the rows and columns corresponding to factor h_i from the reachability matrix. Repeat the above operations to form the final hierarchical structure.

$$L(h_i) = Q(h_i) \cap L(h_i) \quad (20)$$

10. Construct factor association structure. When the value of the i-th row and the j-th column in the reachability matrix is 1, it represents that there is a directional connection between factors i and j, and the directional connection line is drawn according to the result of factor stratification, and the redundant cross-stage transmission path is transitively simplified, and finally the visualization of association relationship is realized.
11. Bayesian network model transformation. Mapping the constructed association structure to Bayesian network, determining the corresponding nodes and directed edges, establishing Bayesian network structure. Obtaining the root node prior probability according to expert experience knowledge, introducing Noisy-orgate model to calculate the conditional probability table of the whole network, and carrying out inference analysis.
12. Association degree calculation. Combined with the inference function of Bayesian network, according to the probability distribution of child nodes before and after the change in parent node state, select "Euclidean" as the distance function [25] to calculate the association degree between nodes.

4. Safety Risk Evolution Model of Hydraulic Tunnel TBM Construction Based on System Dynamics

4.1. Modeling Purposes and System Boundaries

System dynamics focuses on the feedback mechanism formed by the dynamic causal relationships among internal constituent elements, accurately simulating the dynamic characteristics and behaviors of system states over time [26]. Based on the correlation analysis of safety risks in TBM construction of hydraulic tunnels, combined with system dynamics, this paper further explores the evolution trend of safety risks in TBM construction of hydraulic tunnels under the risk correlation situation in the time dimension, analyzes the sensitivity of the overall risk level to the degree of risk correlation, and determines the key factors influencing the changes in the risk level. By understanding the mechanism of risk evolution from multiple dimensions and at a deep level, the scientificity and effectiveness of risk management can be significantly enhanced.

Taking safety risks in hydraulic tunnel TBM construction as the modeling object, the model boundary was defined based on the previously established risk factor system, which consists of five subsystems: geological risk, technical risk, equipment risk, personnel risk, and management risk. In constructing the risk evolution model, two critical dynamic characteristics of the system must be fully considered: time delays and nonlinear relationships.

Time delays refer to situations where a change in one variable does not immediately trigger an instantaneous response in another related variable, but instead occurs after a certain lag period. For example, there is a notable delay between the implementation of safety measures and the actual reduction in risk levels, or between continuous equipment wear and the eventual occurrence of failure. Neglecting such delay effects may lead to misjudgment of the rate of risk development.

Nonlinear relationships indicate that causal effects among variables are not simple proportional correlations, but are instead widely present in complex risk systems. For instance, initial investments in risk management may substantially reduce risk levels, but as investment continues to increase, the marginal benefits of risk reduction may gradually diminish. Conversely, the accumulation of certain risk factors may appear negligible in the early stages but, once surpassing a critical threshold, could result in exponential growth of risk levels.

In this study, delay functions and nonlinear table functions were introduced into the risk evolution model to more accurately capture these complex dynamic behaviors.

4.2. Causal Relationship Diagram

The Causal Relationship Diagram is a conceptual model in system dynamics. It visually presents the influence of effects through causal chains, helping to understand the internal logic of the system. Among them, a positive causal chain refers to the situation where the increase in one variable will correspondingly lead to the increase in another variable, while a negative causal chain means that the directions of change in the two variables are opposite. This article transforms the risk correlation structure into a causal relationship diagram, which greatly resolves the limitations of subjective construction.

4.3. Stock Flow Diagram

The stock flow diagram is a mathematical model in system dynamics, capable of transforming qualitative causal relationships into system stock and flow, and thereby simulating the dynamic changes in the system over time. The basic variables in the stock flow diagram consist of state variables, rate variables, auxiliary variables and constants.

4.4. Model Parameters and Equations

1. Determine the weight of safety risk indicators
   Before constructing and operating the safety risk evolution model for hydraulic tunnel TBM construction, it is necessary to determine the weight values of each index. The weights are calculated by combining subjective and objective methods. The subjective weights are based on the fuzzy DEMATEL method, and the centrality is used to measure the comprehensive importance of each factor in the system. The objective weight calculation adopts the entropy weight method, and the degree of variation is calculated based on the information entropy of the index. Ultimately, the game theory combined weighting method is adopted to coordinate the differences between the subjective and objective weights.

   (1) Fuzzy DEMATEL method to determine subjective weights
   According to the fuzzy DEMATEL calculation method in Section 2.2, the centrality Mi is obtained, and the weight calculation formula is shown in Formula (21).

$$w_i = \frac{M_i}{\sum_{i=1}^{n} M_i} \tag{21}$$

   (2) Entropy weight method to determine objective weight
   The importance of an indicator is determined by information entropy. The greater the information entropy of an indicator, the higher the uncertainty of the data, and its weight relatively decreases. Conversely, the weight is relatively high. The specific calculation process is as follows:

Set m objects and n indexes to construct the original matrix $X^* = (x_{ij})_{m\times n}$, as shown in Formula (22).

$$X^* = \begin{bmatrix} x_{11} & x_{12} & \dots & x_{1n} \\ x_{21} & x_{22} & \dots & x_{2n} \\ \vdots & \vdots & \ddots & \vdots \\ \vdots & \vdots & \dots & \vdots \\ x_{m1} & x_{m2} & \dots & x_{mn} \end{bmatrix} \tag{22}$$

Use Formulae (23) and (24) to dimensionalize indicators of different attributes and standardize the original matrix X^*. For positive indicators:

$$y_{ij} = \frac{x_{ij} - \min\limits_{1\le i\le m}\{x_{ij}\}}{\max\limits_{1\le i\le m}\{x_{ij}\} - \min\limits_{1\le i\le m}\{x_{ij}\}} \tag{23}$$

For negative indicators:

$$y_{ij} = \frac{\max\limits_{1\le i\le m}\{x_{ij}\} - x_{ij}}{\max\limits_{1\le i\le m}\{x_{ij}\} - \min\limits_{1\le i\le m}\{x_{ij}\}} \tag{24}$$

After the processing is completed, the standardized judgment matrix Y^* is obtained, as shown in Formula (25).

$$Y = (y_{ij})_{m\times n} = \begin{bmatrix} y_{11} & y_{12} & \cdots & y_{1n} \\ y_{21} & y_{22} & \cdots & y_{2n} \\ \vdots & \vdots & \ddots & \vdots \\ y_{m1} & y_{m2} & \cdots & y_{mn} \end{bmatrix} \tag{25}$$

According to the basic principle of information entropy, the entropy value e_j^* of the j-th index is calculated from Formulae (26) and (27).

$$r_{ij} = \frac{y_{ij}}{\sum\limits_{i=1}^{m} y_{ij}} (j = 1, 2, \dots, m) \tag{26}$$

$$e_j^* = -\frac{1}{\ln(m)} \sum_{i=1}^{m} r_{ij} \ln(r_{ij}) \tag{27}$$

Then the objective weight W_j^* of the j-th indicator is

$$W_j^* = \frac{1 - e_j^*}{\sum\limits_{j=1}^{n} 1 - e_j^*} \tag{28}$$

(3) Game Theory Combinatorial Weights

The set of weight values calculated by each weight method is $W_k = \{w_{k1}, w_{k2}, \dots, w_{kn}\}(k = 1, 2, \dots, L)$, where L represents the number of weight methods used, n represents the number of indicators, and the combination coefficient is α_k. The calculation formula of comprehensive weight

W_z is shown in (29).

The objective function after optimization of the combination coefficient α_k is shown in Formula (29), and its optimized first-order derivative is transformed into a linear equation system, as shown in Formula (30).

$$W_z = \sum_{k=1}^{L} \alpha_k \cdot W_k^T \tag{29}$$

The objective function after optimization of the combination coefficient α_k is shown in Formula (30), and its optimized first-order derivative is transformed into a linear equation system, as shown in Formula (31).

$$\min \left\| \sum_{k=1}^{L} \alpha_k \cdot W_k^T - W_t^T \right\|_2 (k = 1, 2, \ldots, L) \tag{30}$$

$$\begin{bmatrix} W_1 \cdot W_1^T & W_1 \cdot W_2^T & \ldots & W_1 \cdot W_L^T \\ W_2 \cdot W_1^T & W_2 \cdot W_2^T & \ldots & W_2 \cdot W_L^T \\ \vdots & \vdots & & \vdots \\ W_L \cdot W_1^T & W_L \cdot W_2^T & \ldots & W_L \cdot W_L^T \end{bmatrix} \begin{bmatrix} \alpha_1 \\ \alpha_2 \\ \vdots \\ \alpha_L \end{bmatrix} = \begin{bmatrix} W_1 \cdot W_L^T \\ W_2 \cdot W_2^T \\ \vdots \\ W_L \cdot W_L^T \end{bmatrix} \tag{31}$$

The convergence of the game-theory-based combination weighting method is strictly guaranteed by its mathematical derivation process. The linear system of equations (Formula (31)) originates from the quadratic objective function (Formula (30)), which minimizes the difference between the comprehensive weight vector and the weight vectors obtained from individual weighting methods. Since the Hessian matrix of the objective function is positive definite, the system is ensured to have a unique solution. This unique solution represents the optimal combination coefficients, indicating that the computation process has reached convergence. Subsequently, by normalizing this solution vector (Formula (32)), the final optimal comprehensive weights can be obtained.

$$W' = \sum_{K=1}^{L} \alpha'_k W_k^T \tag{32}$$

2. Determination of risk correlation coefficient
   In the previous section, a risk correlation analysis was conducted based on the fuzzy DEMATEL–ISM–BN approach, where the Euclidean distance function was adopted to calculate the degree of association between nodes. This metric quantifies the absolute magnitude of the influence exerted by a parent node on its child node by computing the Euclidean distance between the child node's probability distribution vectors before and after the parent node's state change. It is particularly suitable for identifying critical influence paths. Compared with measures such as Kullback–Leibler divergence, which emphasize differences in information or relative entropy between probability distributions, Euclidean distance offers greater advantages in intuitively representing the magnitude of influence. Moreover, its computational simplicity ensures analytical efficiency in large-scale networks and facilitates integration with system dynamics models in subsequent analyses.
3. System dynamics equations
   Determine the function expression of each variable in time dimension to quantitatively describe the dynamic interaction among safety risk factors of hydraulic tunnel TBM

construction. According to different variable types, determine the system dynamics equation as shown in Formulae (31)–(35):

$$\text{Rate variable} = \sum(\text{state variable} \times \text{correlation coefficient}) \quad (33)$$

$$\text{State variable} = \text{INTEG (speed variable, initial risk value)} \quad (34)$$

$$\text{Auxiliary variable} = \sum(\text{state variable} \times \text{weight}) \quad (35)$$

4.5. Identification and Handling of Conflicting Causal Chains

In the multi-model framework of this study, potential conflicting causal links were systematically addressed through a multi-stage process. First, during the fuzzy DEMATEL analysis stage, consensus among experts was facilitated by means of a modified Delphi method, thereby resolving expert opinion conflicts in causal judgments. Second, in the construction of the static correlation network, the hierarchical decomposition mechanism of the Interpretive Structural Modeling (ISM) method was applied to transform the network into a directed acyclic hierarchical structure, which resolved structural loop conflicts that could not be accommodated by the static model, and distilled the backbone causal pathways of the system. Finally, at the stage of dynamic evolution, the System Dynamics (SD) model was specifically employed to construct and simulate critical feedback loops. Based on the unidirectional backbone causal chains identified by the ISM–BN model, the SD model further introduced realistic bidirectional causal relationships, thereby ensuring high fidelity in the final dynamic simulations.

More specifically, the ISM–BN model, through its hierarchical structuring and causal chain analysis, revealed the unidirectional influence pathways among risk factors, which served as the foundation for feedback loop identification in the SD model. At the SD modeling stage, these unidirectional chains identified by the ISM–BN analysis were carefully reviewed and extended using domain expert knowledge and practical engineering experience, in order to identify potential bidirectional interactions. For example, if factor A was shown by the ISM–BN analysis to have a unidirectional influence on factor B, while in practice factor B might also exert an effect back on factor A, the SD model incorporated this bidirectional interaction as a feedback loop, thereby enabling a more realistic simulation of risk evolution. This sequential process ensured an effective transition from an initially complex and potentially conflicting understanding to a logically rigorous and dynamically faithful simulation model.

4.6. Model Operation and Analysis

After the above parameters and equations are constructed, they are input into the simulation software Vensim PLE7.3.5 to start the simulation. After successful operation, sensitivity analysis can be carried out by adjusting the parameters to determine the key subsystems and key factors.

5. Example Analysis

5.1. Project Overview

The AY hydraulic tunnel project undertakes the important task of meeting the local production and living water demands, achieving the rational and efficient allocation of water resources. It consists of four parts: the drilling and blasting section, the TBM starting section, the TBM tunneling section and the receiving section. Among them, the TBM tunneling section is constructed using a double-shield TBM, with a length of 11.822 km. The geological conditions along the alignment of the hydraulic tunnel are highly complex, traversing composite strata and intersecting multiple natural fault zones. The tunnel passes

successively through goaf areas, faults, karst zones, and other unfavorable geological sections. In addition, the alignment crosses several mountain gullies, where severe weathering has led to loose rock structures. In shallow-buried sections, the tunnel crown is often surrounded by Class V rock mass with poor stability, making it highly susceptible to rockfalls and collapses. During the rainy season, water accumulation may trigger inrush events, further threatening construction safety. Although groundwater levels are relatively low in most sections of the tunnel, certain segments near rivers have undergone long-term erosion, resulting in karst caves that substantially reduce rock mass stability. Moreover, surface infiltration and fissure water may cause leakage and dripping during excavation, exerting adverse effects on both construction quality and progress. The geological features and construction techniques of this project are highly representative and have certain reference value for similar TBM construction projects.

5.2. Correlation Analysis of Safety Risks in Hydraulic Tunnel TBM Construction

5.2.1. Risk Factor Analysis Based on Fuzzy DEMATEL

Invite 10 experts and scholars from research institutes and universities who are engaged in the safety management and risk management of hydraulic structure construction and other related fields, as well as technical backbones from the front line of TBM construction projects. Fully combine the geological exploration data, construction plans, construction parameters and other types of data of this project In accordance with standards such as the "Technical Code for TBM Construction of Hydraulic Tunnels" (TCCIAT0030-2020) and the "Technical Specifications for TBM Construction of Hydraulic Tunnels" (T/CPPC1106-2025), the degree of influence among factors is scored based on the five grades set in the previous text. Refer to Table 2 to convert the language variables in the collected initial scoring matrix to the corresponding triangular fuzzy numbers, and calculate the comprehensive influence matrix D using Formulae (3)–(13).

$$D = \begin{bmatrix}
0.0347 & 0.0347 & 0.1407 & 0.1176 & 0.0498 & 0.0433 & 0.1114 & 0.0542 & 0.0553 & 0.0384 & 0.1257 & 0.0850 & 0.1438 & 0.0472 & 0.0417 & 0.0386 & 0.0492 & 0.0347 & 0.0369 & 0.0418 & 0.0371 \\
0.0337 & 0.0337 & 0.1236 & 0.1115 & 0.0484 & 0.0420 & 0.1243 & 0.0525 & 0.0537 & 0.0372 & 0.1181 & 0.1055 & 0.0896 & 0.0458 & 0.0405 & 0.0375 & 0.0477 & 0.0337 & 0.0358 & 0.0406 & 0.0360 \\
0.0297 & 0.0297 & 0.0504 & 0.0476 & 0.0427 & 0.0371 & 0.1028 & 0.0464 & 0.0474 & 0.0329 & 0.1167 & 0.0474 & 0.1118 & 0.0405 & 0.0357 & 0.0331 & 0.0421 & 0.0297 & 0.0316 & 0.0358 & 0.0318 \\
0.0308 & 0.0308 & 0.0522 & 0.0493 & 0.0442 & 0.0384 & 0.0934 & 0.0480 & 0.0490 & 0.0340 & 0.1143 & 0.1043 & 0.1150 & 0.0419 & 0.0370 & 0.0342 & 0.0436 & 0.0308 & 0.0328 & 0.0371 & 0.0329 \\
0.0335 & 0.0335 & 0.1165 & 0.1179 & 0.0481 & 0.0418 & 0.1082 & 0.0523 & 0.0534 & 0.0370 & 0.1245 & 0.0788 & 0.1183 & 0.0456 & 0.0403 & 0.0373 & 0.0474 & 0.0335 & 0.0357 & 0.0404 & 0.0358 \\
0.0384 & 0.0384 & 0.1224 & 0.1072 & 0.0552 & 0.0479 & 0.1401 & 0.1307 & 0.1386 & 0.0425 & 0.1401 & 0.0980 & 0.1535 & 0.0523 & 0.0462 & 0.0428 & 0.0544 & 0.0384 & 0.0409 & 0.0463 & 0.0411 \\
0.0255 & 0.0255 & 0.0432 & 0.0408 & 0.0366 & 0.0318 & 0.0464 & 0.0397 & 0.0406 & 0.0282 & 0.0469 & 0.0406 & 0.0475 & 0.0347 & 0.0306 & 0.0283 & 0.0361 & 0.0255 & 0.0271 & 0.0307 & 0.0272 \\
0.0310 & 0.0310 & 0.1101 & 0.1028 & 0.0445 & 0.0386 & 0.0809 & 0.0483 & 0.0494 & 0.0342 & 0.0912 & 0.0699 & 0.0838 & 0.0422 & 0.0372 & 0.0345 & 0.0439 & 0.0310 & 0.0330 & 0.0373 & 0.0331 \\
0.0289 & 0.0289 & 0.1067 & 0.0463 & 0.0415 & 0.0361 & 0.0840 & 0.0451 & 0.0461 & 0.0320 & 0.0765 & 0.0461 & 0.0769 & 0.0394 & 0.0348 & 0.0322 & 0.0410 & 0.0289 & 0.0308 & 0.0349 & 0.0309 \\
0.0373 & 0.0373 & 0.0966 & 0.0849 & 0.1177 & 0.0464 & 0.1004 & 0.1246 & 0.1257 & 0.0412 & 0.1230 & 0.1097 & 0.1384 & 0.0507 & 0.0448 & 0.0414 & 0.0527 & 0.0373 & 0.0396 & 0.0449 & 0.0398 \\
0.0255 & 0.0255 & 0.0432 & 0.0408 & 0.0366 & 0.0318 & 0.0464 & 0.0397 & 0.0406 & 0.0282 & 0.0469 & 0.0406 & 0.0475 & 0.0347 & 0.0306 & 0.0283 & 0.0361 & 0.0255 & 0.0271 & 0.0307 & 0.0272 \\
0.0255 & 0.0255 & 0.0432 & 0.0408 & 0.0366 & 0.0318 & 0.0464 & 0.0397 & 0.0406 & 0.0282 & 0.0469 & 0.0406 & 0.0475 & 0.0347 & 0.0306 & 0.0283 & 0.0361 & 0.0255 & 0.0271 & 0.0307 & 0.0272 \\
0.0255 & 0.0255 & 0.0432 & 0.0408 & 0.0366 & 0.0318 & 0.0464 & 0.0397 & 0.0406 & 0.0282 & 0.0469 & 0.0406 & 0.0475 & 0.0347 & 0.0306 & 0.0283 & 0.0361 & 0.0255 & 0.0271 & 0.0307 & 0.0272 \\
0.0333 & 0.0333 & 0.0782 & 0.0806 & 0.0478 & 0.0415 & 0.0785 & 0.1116 & 0.1083 & 0.0368 & 0.0845 & 0.1131 & 0.1023 & 0.0453 & 0.0400 & 0.0370 & 0.0471 & 0.0333 & 0.0354 & 0.0401 & 0.0356 \\
0.0414 & 0.0414 & 0.1052 & 0.0945 & 0.1127 & 0.1048 & 0.1167 & 0.1249 & 0.1331 & 0.0990 & 0.1292 & 0.0944 & 0.1286 & 0.1051 & 0.0498 & 0.0461 & 0.1119 & 0.0414 & 0.0441 & 0.0499 & 0.0443 \\
0.0414 & 0.0414 & 0.1007 & 0.1028 & 0.1166 & 0.1070 & 0.1391 & 0.1185 & 0.1443 & 0.0458 & 0.1301 & 0.0980 & 0.1139 & 0.1205 & 0.0497 & 0.0461 & 0.1206 & 0.0414 & 0.0441 & 0.0499 & 0.0442 \\
0.0392 & 0.0392 & 0.1223 & 0.1035 & 0.1205 & 0.0489 & 0.1545 & 0.1297 & 0.1289 & 0.0433 & 0.1154 & 0.1092 & 0.1420 & 0.0533 & 0.0471 & 0.0436 & 0.0555 & 0.0392 & 0.0417 & 0.0472 & 0.0419 \\
0.0507 & 0.0507 & 0.1260 & 0.1242 & 0.1349 & 0.0977 & 0.1483 & 0.1323 & 0.1333 & 0.0705 & 0.1430 & 0.1322 & 0.1399 & 0.1360 & 0.1296 & 0.1048 & 0.1611 & 0.0507 & 0.1182 & 0.1443 & 0.1229 \\
0.0478 & 0.0478 & 0.1216 & 0.1217 & 0.1049 & 0.1201 & 0.1521 & 0.1224 & 0.1197 & 0.0720 & 0.1432 & 0.1125 & 0.1594 & 0.1503 & 0.1283 & 0.1174 & 0.1405 & 0.0478 & 0.0509 & 0.1218 & 0.0511 \\
0.0396 & 0.0396 & 0.0987 & 0.1010 & 0.1241 & 0.0494 & 0.1288 & 0.1048 & 0.1100 & 0.0438 & 0.1174 & 0.0969 & 0.1122 & 0.1269 & 0.0476 & 0.0441 & 0.1379 & 0.0396 & 0.0422 & 0.0477 & 0.0423 \\
0.0400 & 0.0400 & 0.0946 & 0.0992 & 0.0884 & 0.0929 & 0.1053 & 0.0987 & 0.1030 & 0.0627 & 0.1100 & 0.0972 & 0.1147 & 0.0771 & 0.1101 & 0.0445 & 0.1134 & 0.0400 & 0.0426 & 0.1058 & 0.0428
\end{bmatrix}$$

(1) Using the comprehensive influence matrix D and combining Formulae (14)–(17), calculate the influence degree e_i, affected degree f_i, center degree M_i and cause degree N_i of each risk index. The calculation results are shown in Table 5.

(2) According to the above calculation results, draw a risk index causality diagram with centrality as horizontal axis and causation as vertical axis, as shown in Figure 3. Centrality indicates the comprehensive influence of factors in the system, and the larger the value, the more significant the overall influence of the factor on the system; when the causation degree is positive, it is classified as cause factor, indicating that the factor has greater influence on other factors, and vice versa, it is classified as result factor.

Table 5. Parameter results of fuzzy DEMATEL analysis.

Risk Factor	Influence Degree e_i	Affected Degree f_i	Centrality M_i	Degree of Causation N_i	Centrality Sort	Factor Attributes
X_{11}	1.3618	0.7334	2.0952	0.6284	20	Causative factor
X_{12}	1.2914	0.7334	2.0248	0.558	21	Causative factor
X_{13}	1.0229	1.9393	2.9622	−0.9164	4	Outcome factor
X_{14}	1.094	1.7758	2.8698	−0.6818	9	Outcome factor
X_{21}	1.2798	1.4884	2.7682	−0.2086	13	Outcome factor
X_{22}	1.6154	1.1611	2.7765	0.4543	12	Causative factor
X_{23}	0.7335	2.1544	2.8879	−1.4209	8	Outcome factor
X_{24}	1.1079	1.7038	2.8117	−0.5959	10	Outcome factor
X_{25}	0.968	1.7616	2.7296	−0.7936	15	Outcome factor
X_{31}	1.5344	0.9161	2.4505	0.6183	19	Causative factor
X_{32}	0.7335	2.1905	2.924	−1.457	6	Outcome factor
X_{33}	0.7335	1.7606	2.4941	−1.0271	18	Outcome factor
X_{34}	0.7335	2.2341	2.9676	−1.5006	4	Outcome factor
X_{35}	1.2636	1.3589	2.6225	−0.0953	16	Outcome factor
X_{41}	1.8185	1.0828	2.9013	0.7357	7	Causative factor
X_{42}	1.8161	0.9284	2.7445	0.8877	14	Causative factor
X_{43}	1.6661	1.4544	3.1205	0.2117	2	Causative factor
X_{51}	2.4513	0.7334	3.1847	1.7179	1	Causative factor
X_{52}	2.2533	0.8447	3.098	1.4086	3	Causative factor
X_{53}	1.6946	1.0886	2.7832	0.606	11	Causative factor
X_{54}	1.723	0.8524	2.5754	0.8706	17	Causative factor

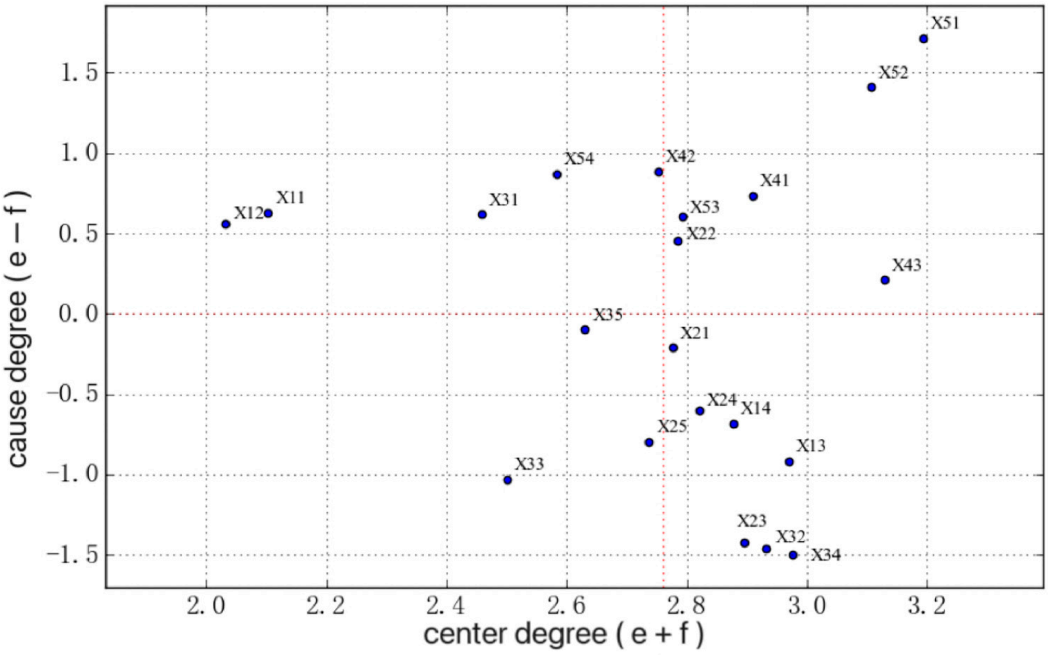


Figure 3. Causality diagram of risk indicators.

In the horizontal dimension, elements with larger centrality values are distributed further to the right, including X_{51}, X_{52}, X_{43}, X_{34}, etc. These nodes have a strong influence in the network and threaten the construction safety of the tunnel from multiple aspects. As can be seen from Table 5 and Figure 3, there are a total of 11 cause factors. Among them, the top 5 in terms of cause degree are: incomplete management system, failure to implement safety training and technical briefings, weak safety awareness, unreasonable personnel allocation and insufficient technical level. Implementing targeted preventive measures for these cause factors can achieve the source blocking of construction safety risk governance.

5.2.2. Construction of Risk Correlation Structure Based on ISM

Using the comprehensive influence matrix D, the overall influence matrix O is obtained by using Formula (18). The appropriate threshold λ is selected for multiple calculations, and finally the sum of the mean and standard deviation of the comprehensive influence matrix D is used as the threshold λ. After screening and optimization, the reachable matrix K is obtained.

$$K = \begin{bmatrix}
1 & 0 & 1 & 1 & 0 & 0 & 1 & 0 & 0 & 0 & 1 & 0 & 1 & 0 & 0 & 0 & 0 & 0 & 0 & 0 & 0 \\
0 & 1 & 1 & 1 & 0 & 0 & 1 & 0 & 0 & 0 & 1 & 1 & 0 & 0 & 0 & 0 & 0 & 0 & 0 & 0 & 0 \\
0 & 0 & 1 & 0 & 0 & 0 & 0 & 0 & 0 & 0 & 1 & 0 & 1 & 0 & 0 & 0 & 0 & 0 & 0 & 0 & 0 \\
0 & 0 & 0 & 1 & 0 & 0 & 0 & 0 & 0 & 0 & 1 & 1 & 1 & 0 & 0 & 0 & 0 & 0 & 0 & 0 & 0 \\
0 & 0 & 1 & 1 & 1 & 0 & 1 & 0 & 0 & 0 & 1 & 0 & 1 & 0 & 0 & 0 & 0 & 0 & 0 & 0 & 0 \\
0 & 0 & 1 & 1 & 0 & 1 & 1 & 1 & 1 & 0 & 1 & 0 & 1 & 0 & 0 & 0 & 0 & 0 & 0 & 0 & 0 \\
0 & 0 & 0 & 0 & 0 & 0 & 1 & 0 & 0 & 0 & 0 & 0 & 0 & 0 & 0 & 0 & 0 & 0 & 0 & 0 & 0 \\
0 & 0 & 1 & 0 & 0 & 0 & 0 & 1 & 0 & 0 & 0 & 0 & 0 & 0 & 0 & 0 & 0 & 0 & 0 & 0 & 0 \\
0 & 0 & 1 & 0 & 0 & 0 & 0 & 0 & 1 & 0 & 0 & 0 & 0 & 0 & 0 & 0 & 0 & 0 & 0 & 0 & 0 \\
0 & 0 & 0 & 0 & 1 & 0 & 0 & 1 & 1 & 1 & 1 & 1 & 1 & 0 & 0 & 0 & 0 & 0 & 0 & 0 & 0 \\
0 & 0 & 0 & 0 & 0 & 0 & 0 & 0 & 0 & 0 & 1 & 0 & 0 & 0 & 0 & 0 & 0 & 0 & 0 & 0 & 0 \\
0 & 0 & 0 & 0 & 0 & 0 & 0 & 0 & 0 & 0 & 0 & 1 & 0 & 0 & 0 & 0 & 0 & 0 & 0 & 0 & 0 \\
0 & 0 & 0 & 0 & 0 & 0 & 0 & 0 & 0 & 0 & 0 & 0 & 1 & 0 & 0 & 0 & 0 & 0 & 0 & 0 & 0 \\
0 & 0 & 0 & 0 & 0 & 0 & 0 & 1 & 1 & 0 & 0 & 1 & 0 & 1 & 0 & 0 & 0 & 0 & 0 & 0 & 0 \\
0 & 0 & 1 & 0 & 1 & 1 & 1 & 1 & 1 & 0 & 1 & 0 & 1 & 1 & 1 & 0 & 1 & 0 & 0 & 0 & 0 \\
0 & 0 & 0 & 0 & 1 & 1 & 1 & 1 & 1 & 0 & 1 & 0 & 1 & 1 & 0 & 1 & 1 & 0 & 0 & 0 & 0 \\
0 & 0 & 1 & 1 & 1 & 0 & 1 & 1 & 1 & 0 & 1 & 1 & 1 & 0 & 0 & 0 & 1 & 0 & 0 & 0 & 0 \\
0 & 0 & 1 & 1 & 1 & 0 & 1 & 1 & 1 & 0 & 1 & 1 & 1 & 1 & 1 & 1 & 1 & 1 & 1 & 1 & 1 \\
0 & 0 & 1 & 1 & 1 & 1 & 1 & 1 & 1 & 0 & 1 & 1 & 1 & 1 & 1 & 1 & 1 & 0 & 1 & 1 & 0 \\
0 & 0 & 0 & 0 & 1 & 0 & 1 & 1 & 1 & 0 & 1 & 0 & 1 & 1 & 0 & 0 & 1 & 0 & 0 & 1 & 0 \\
0 & 0 & 0 & 0 & 0 & 0 & 1 & 0 & 0 & 0 & 1 & 0 & 1 & 0 & 1 & 0 & 1 & 0 & 0 & 1 & 1
\end{bmatrix}$$

According to the reachability matrix hierarchy analysis procedure described above, combined with matrix K, risk factors are divided into 7 levels, the first level is $L_1 = \{X_{23}, X_{32}, X_{33}, X_{34}\}$, the second level is $L_2 = \{X_{13}, X_{14}\}$, the third level is $L_3 = \{X_{11}, X_{12}, X_{21}, X_{24}, X_{25}\}$, the fourth level is $L_4 = \{X_{22}, X_{31}, X_{35}, X_{43}\}$, the fifth level is $L_5 = \{X_{41}, X_{42}, X_{53}\}$, the sixth level is $L_6 = \{X_{52}, X_{54}\}$, and the seventh level is $L_7 = \{X_{51}\}$. Each level is further divided into root factors, transition factors and surface factors according to the meaning and expression form of factors. Root factors include factors at levels 5, 6 and 7, transition factors include factors at levels 3 and 4, and surface factors include factors at levels 1 and 2. Directed connection lines are drawn in combination with the position of "1" in the reachability matrix K, and redundant cross-level transmission paths are removed for transitivity simplification to finally determine the risk association structure, as shown in Figure 4.

The specific analysis of the three levels of safety risk factors is as follows:

(1) The root factors include X_{51}, X_{52}, X_{54}, X_{41}, etc., which are the initial causes that trigger the associated transmission of risks and affect construction safety. Prioritizing the control of root causes before construction can reduce risks at the lowest cost.

(2) Transition factors are the key intermediate links in the process of risk correlation transmission, which play the role of risk amplification or buffer, mainly manifested as technical risk factors.

(3) Surface factors refer to specific events or phenomena that cause actual losses such as safety accidents and construction halts after the associated transmission of risks, such

as specific abnormal issues like X_{32}, X_{34}, X_{23}, and X_{33}. For instance, the instability and deformation of the surrounding rock of X13 not only directly threaten the lives and safety of personnel, but also can cause the shield to get stuck or the excavation to deviate from the axis. The characteristics of surface factors are directness, observability and urgency, and they can be controlled through real-time monitoring and emergency measures.

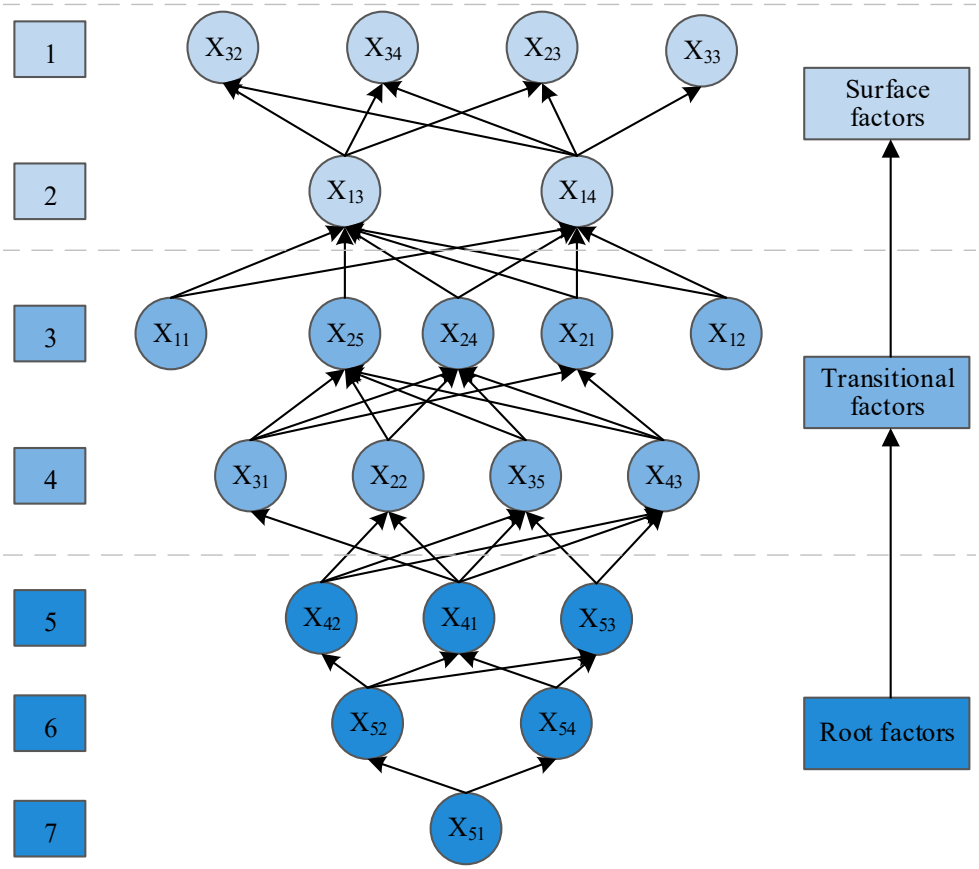


Figure 4. Safety risk associated structure of TBM construction in hydraulic tunnel.

5.2.3. Calculation of Risk Correlation Degree Based on ISM–BN

Based on the constructed safety risk association structure of the hydraulic tunnel TBM construction, it is mapped into a Bayesian network topology structure, with the interaction relationships of each node corresponding one-to-one. At the top layer, the safety risk of the hydraulic tunnel TBM construction is added as a leaf node, the risk factor at the 7th layer is mapped as the root node, and the risk factors at the remaining levels are mapped as intermediate nodes. The action paths of risk factors are mapped to directed edges, and the states of each node are defined, respectively, where Y represents the probability of risk occurrence and N represents the probability of risk non-occurrence.

(1) Positive causal reasoning

Based on the discussion in Section 3.3, the occurrence probabilities of risk factors were assessed by integrating expert knowledge, historical experience, TBM construction case data, and professional expertise. According to the prior probability grading criteria for root nodes and the corresponding fuzzy numbers, experts' natural language evaluations were processed using Formulae (4) and (11). This yielded the prior probabilities for root nodes including X11 adverse geological conditions, X_{12} unfavorable hydrogeological conditions, and X_{51} inadequate management systems. For non-root nodes, the Noisy-or gate model was employed to calculate the probability

of child nodes occurring under any given parent node state, thereby generating the conditional probability tables (CPTs).

In the GeNIe4.1.3402 software, the calculated probability parameters were input into the corresponding nodes of the Bayesian network (BN) model for safety risk analysis of hydraulic tunnel TBM construction, completing the parameter learning process. Through forward causal inference, the posterior probability distributions of 18 risk factors were obtained. The occurrence probability data of all factors were then exported and summarized, with the inference results presented in Figure 5.

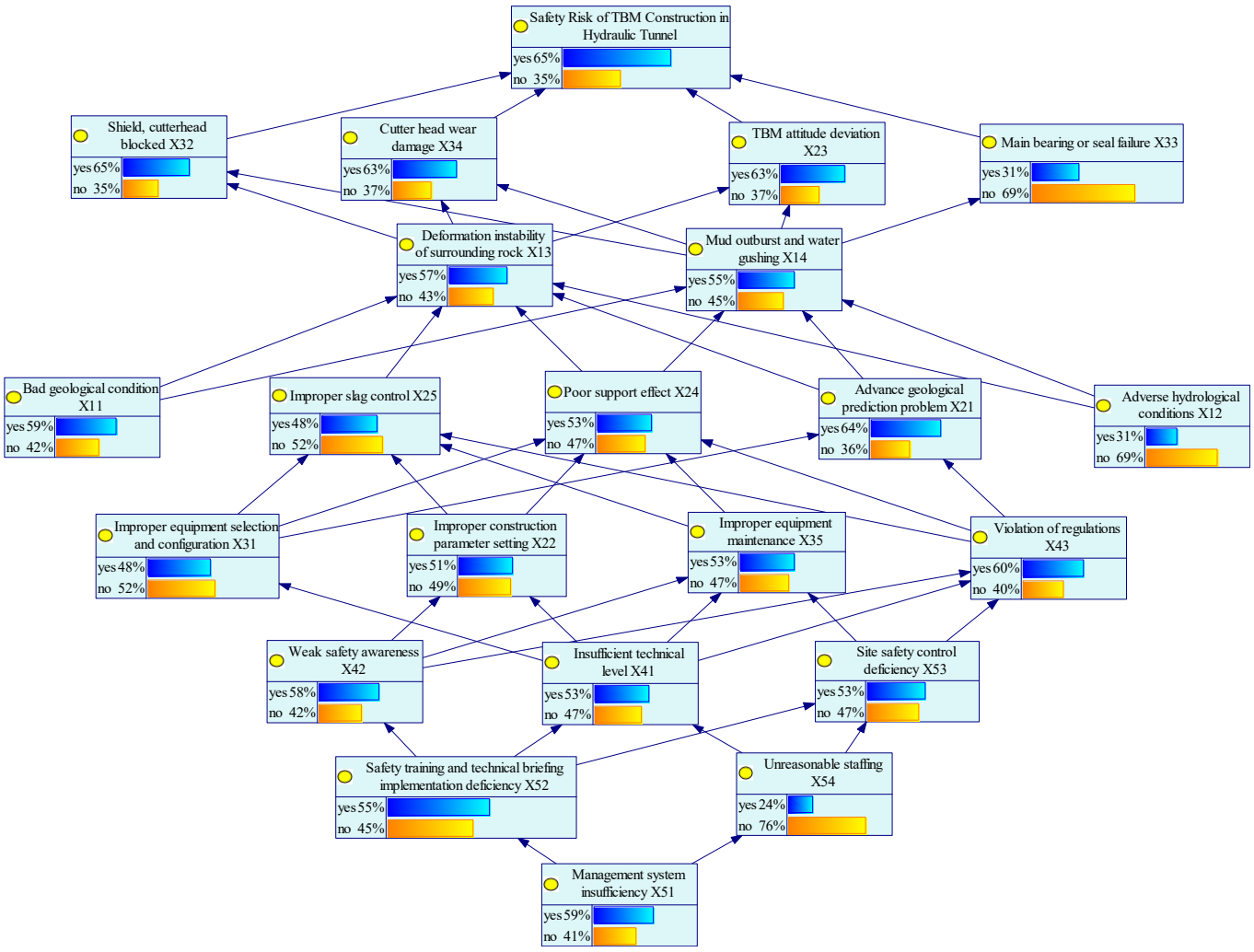


Figure 5. Positive reasoning results of Bayesian network.

The forward inference results of the model indicate that the probability of construction safety risk occurrence in the AY project is 0.6517, with 77% of the node probabilities falling within the range of 0.5–0.7. This value suggests that the system operates at a relatively high risk level. Among the root risks, inadequate management systems (X_{51}) exhibited the highest risk index, approximately 0.59, implying that it may represent a major contributor to the overall system risk. These indices provide a quantitative basis for identifying critical risk domains. Among non-leaf nodes, the basic event corresponding to the minimum occurrence probability of 0.239 is unreasonable staffing of X_{54}, which is consistent with the actual staffing situation of the project and meets the construction requirements. However, the occurrence probability of violations is relatively high, and training and supervision efforts still need to be continuously

increased. The maximum value of X_{34} cutterhead and shield blocked is 0.6494, which is affected by the actual geological conditions of the project. The TBM construction area of AY Project includes shallow buried and highly weathered sections and fault fracture zones, which is easy to cause collapse and block loss, resulting in TBM jamming. Geological prediction shall be strengthened during construction, and preventive measures such as advance grouting shall be taken to fully deal with the tunnel sections under adverse conditions.

(2) Degree of association calculation

Referring to step (9) in Section 3.3, the Euclidean function is used in the GeNIe software to calculate the degree of association between factors, and the results are visually expressed through the thickness of the transfer path. The width of the directed edge represents the degree of association. The wider the line, the greater the degree of association, as shown in Figure 6. Encode the risk association path. For example, when X_{13} is passed to X_{23}, it becomes "TF1113". The specific association degree values are shown in Table 6. From the analysis of the calculation results, it can be seen that the most significant correlation is between the incomplete management system of X_{51} and the failure to implement safety training and technical briefings of X_{52}, representing the close connection between the two.

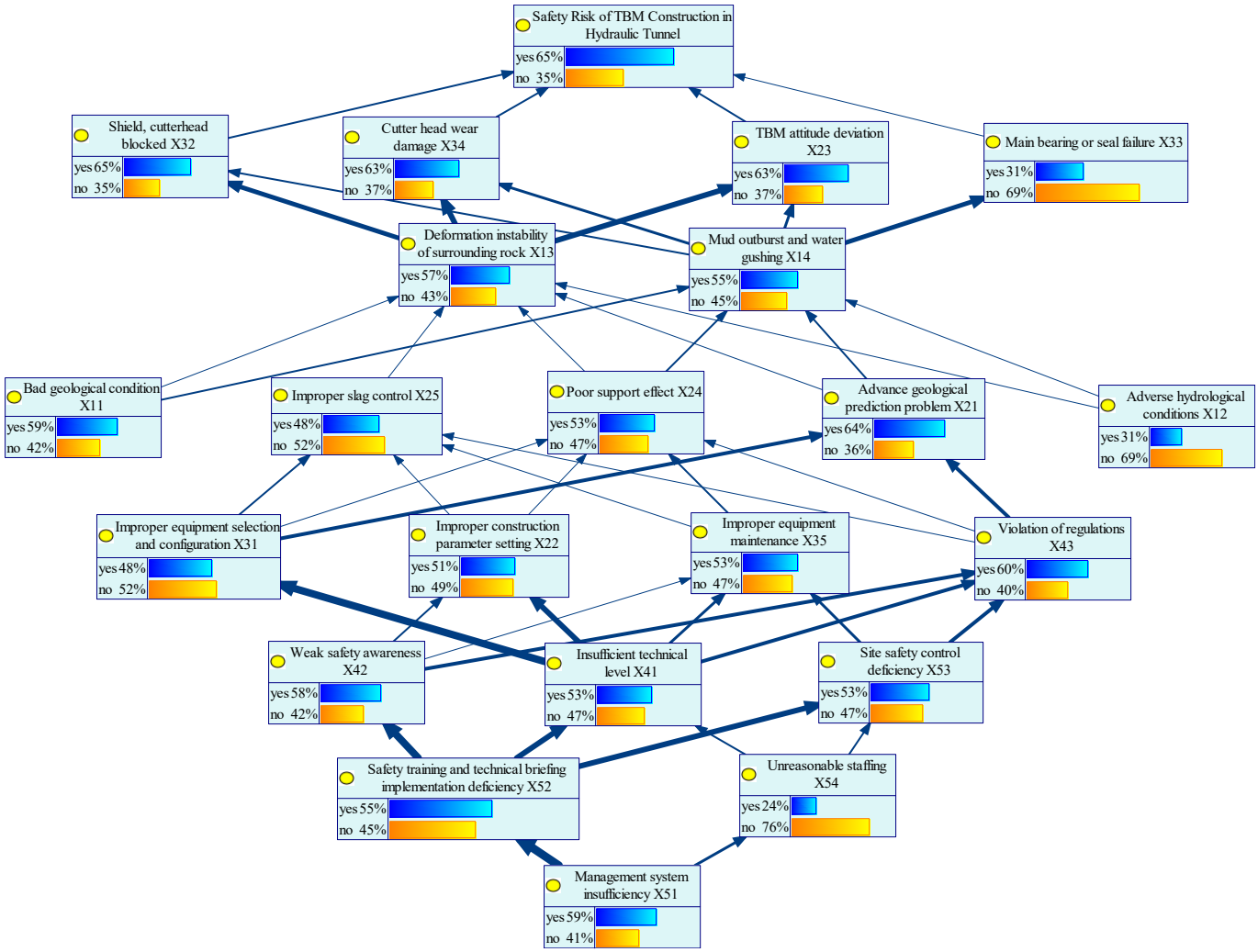


Figure 6. Calculation results of the correlation degree of Bayesian network.

Table 6. Safety risk correlation degree of TBM construction in hydraulic tunnel.

Associated Path	Association Degree	Associated Path	Association Degree
TF1113	0.198	TF3524	0.253
TF1114	0.244	TF3525	0.169
TF1213	0.166	TF4122	0.685
TF1214	0.193	TF4131	0.786
TF1323	0.636	TF4135	0.352
TF1332	0.594	TF4143	0.490
TF1334	0.611	TF4222	0.296
TF1423	0.302	TF4235	0.158
TF1432	0.261	TF4243	0.490
TF1433	0.549	TF4321	0.420
TF1434	0.307	TF4324	0.169
TF2113	0.198	TF4325	0.169
TF2114	0.244	TF5152	0.812
TF2224	0.169	TF5154	0.388
TF2225	0.169	TF5241	0.596
TF2413	0.198	TF5242	0.793
TF2414	0.244	TF5253	0.593
TF2513	0.106	TF5335	0.352
TF3121	0.472	TF5343	0.490
TF3124	0.179	TF5441	0.370
TF3125	0.253	TF5453	0.266

5.2.4. Validation of Bayesian Network Probabilities

To ensure the rationality of the probability parameters and the validity of the final inference results in the Bayesian network (BN) model, a multi-stage validation strategy was employed, systematically examining the model from three perspectives: structure, input parameters, and output results.

1. Structural logic validation.
   The structure of the BN (i.e., the causal relationships among risk factors) was not arbitrarily defined but was strictly derived from the hierarchical model established through fuzzy DEMATEL and ISM analysis. The ISM method itself, based on rigorous matrix operations, guarantees logical consistency of the constructed causal pathways and the absence of cyclic loops. This systematic structural modeling process provided a validated logical framework for subsequent probability assignments and represents the first step in probability validation.
2. Cross-validation and convergence testing of input parameters.
   The input probabilities of the model, including prior probabilities for root nodes and conditional probability tables (CPTs), were primarily derived from expert knowledge. To ensure their reliability, the following measures were taken:
   (1) Consensus on prior probabilities. The prior probabilities of root nodes (e.g., X_{51} —inadequate management systems) were not determined by a simple average of one-time expert ratings. Instead, a modified Delphi method was adopted, incorporating multiple rounds of anonymous feedback and statistical analysis to guide the expert group toward consensus. This ensured convergence and stability of the input values and effectively reduced the impact of individual biases.
   (2) Simplification and validation of conditional probabilities. Given the difficulty and error-proneness of directly eliciting large CPTs, this study applied the widely used Noisy-or gate model in risk analysis. This model decomposes complex conditional probabilities into a set of single-causal influence probabilities that are easier for experts to understand and assess, thus reduc-

ing cognitive load. During parameterization, experts were invited to evaluate the "leak probabilities" and "causal influence strengths" of key nodes, and cross-checking was conducted to validate the internal consistency of their assessments.

3. Validation of output results.
Upon model construction and forward inference, the posterior probability results (see Figure 6) were subjected to validity checks:

(1) Comparison with real project data. The model outputs—particularly high-probability risk nodes (e.g., X_{34}—cutterhead wear and damage, probability = 0.6494) and critical influence paths—were compared with the AY project's construction logs, technical meeting minutes, and interviews with site engineers. The results demonstrated high consistency between the identified risks and the actual challenges encountered in practice (e.g., severe cutterhead wear and TBM jamming during excavation through shallow-buried, heavily weathered strata and fault fracture zones). This consistency with real-world conditions provides strong macro-level validation of the model outputs.

(2) Scenario analysis and sensitivity testing. "What-if" scenarios were designed to examine the logical responsiveness of the model. For instance, when the probability of "X_{51}—inadequate management systems" was artificially set to a very low value (simulating an ideal management condition), the downstream risks such as "X_{52}—insufficient safety training" and "X_{54}—unreasonable personnel allocation" showed significant probability reductions, ultimately lowering the overall system risk level. The model's behavior fully aligned with logical expectations, thereby validating the reasonableness of probability propagation throughout the network from a dynamic perspective.

Finally, it is important to emphasize that since the input parameters were derived mainly from expert judgment rather than large-scale frequency statistics, the model outputs should be interpreted as a Risk Index or Relative Metric rather than absolute probabilities of occurrence. The primary value of the BN model lies in supporting trend analysis, key risk identification, and scenario comparison, rather than providing exact objective probability predictions. Through this multi-dimensional validation process, the BN model and its probability parameters are shown to offer reliable and insightful decision support for safety risk management in hydraulic tunnel TBM construction.

5.3. Simulation Analysis of Safety Risk Evolution in TBM Construction of Hydraulic Tunnels

5.3.1. Causality Diagram Establishment

According to the determined system boundary and association structure, the causal relationship of risk factors within each subsystem and among subsystems is obtained, the subsystems are divided in turn, and the causal relationship diagram of total system safety risk of hydraulic tunnel TBM construction is drawn by Vensim software, as shown in Figure 7.

5.3.2. Establishment of the Stock Flow Diagram

To further analyze the evolution trend of safety risks in TBM construction of hydraulic tunnels, combined with system requirements, based on the causal relationship diagram, the risk level L_{xy} of factors in each subsystem is set as the state variable, and the risk level increment Rt_{xy} is set as the rate variable. The overall system risk level L and the risk levels $L_{1–5}$ of each subsystem are auxiliary variables. According to the numbering in the safety risk indicator system for hydraulic tunnel TBM construction, the factors were encoded, and

a stock–flow diagram of safety risks in hydraulic tunnel TBM construction was developed using Vensim software, as shown in Figure 8.

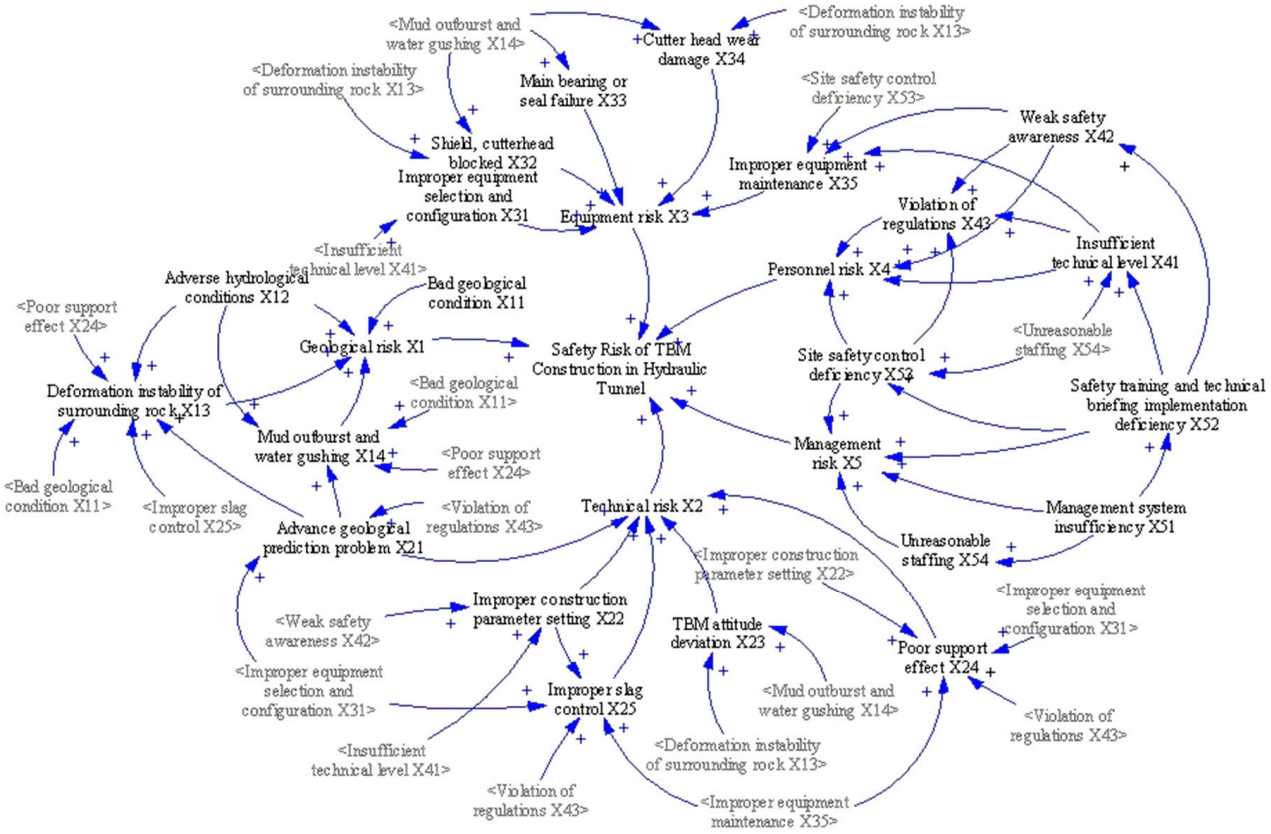


Figure 7. Causal relationship diagram of the overall safety risk system in hydraulic tunnel TBM construction.

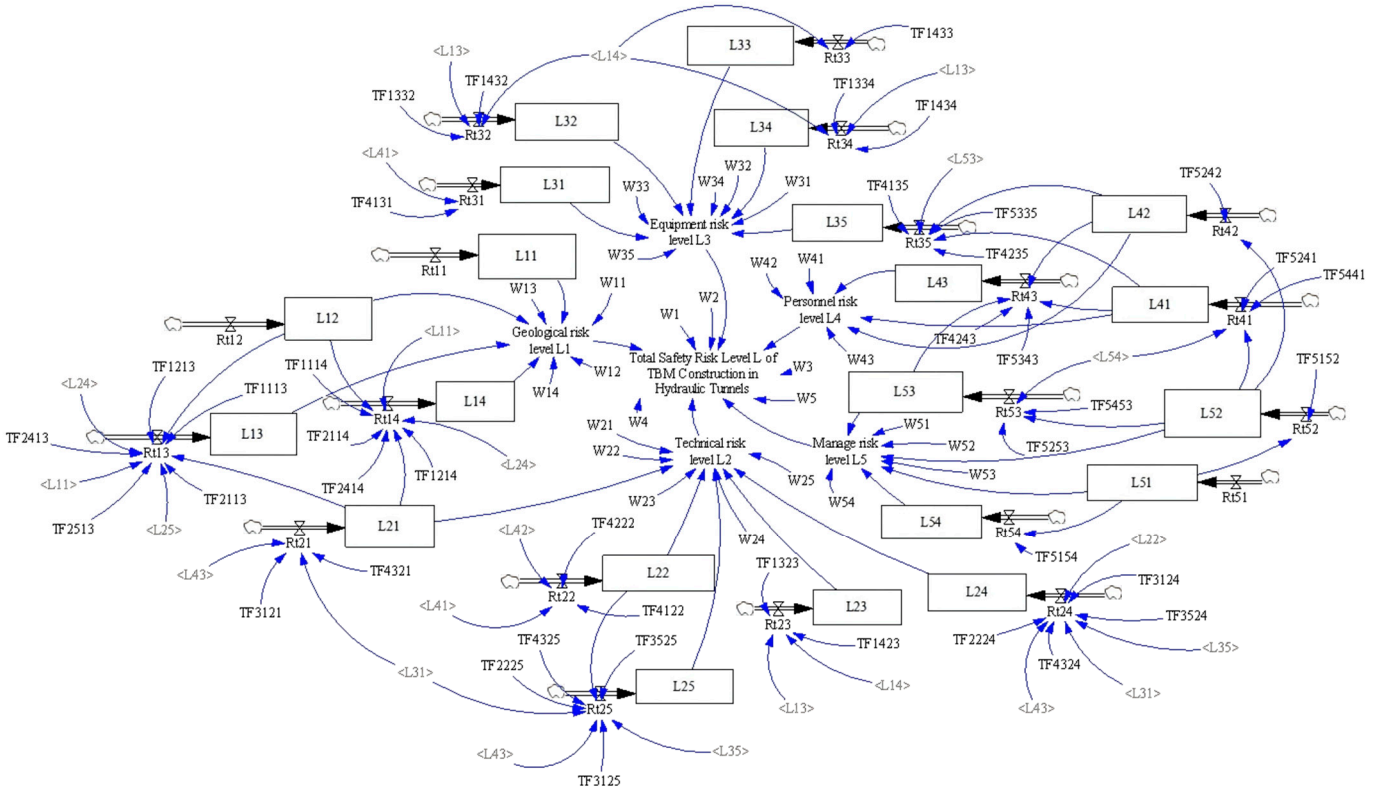


Figure 8. Safety risk stock flow diagram of hydraulic tunnel TBM construction.

5.3.3. Model Parameter Determination

(1) Index weight calculation

Firstly, based on the centrality values calculated by the fuzzy DEMATEL analysis in Table 5, the subjective weights of the indicators are calculated using Formula (21). Secondly, the entropy weight method was used to determine the objective weights. Five management and technical personnel who were familiar with or had participated in this construction project were invited to discuss and score the safety impact degree of each risk factor based on the collected TBM construction logs and tunneling parameter records of the AY project. The corresponding scale for the evaluation grade values was [1–5]. The higher the score, the greater the harm caused by the risk factors. The objective weights are determined according to Formulae (22)–(28). Finally, calculate the combined weighting results of game theory according to Formulae (29)–(31). The subjective, objective and combined weights of all indicators are shown in Table 7.

Table 7. Weights of risk indicator combinations.

First-Level Index	Fuzzy DEMATEL Method	Entropy Weight Method	Combinatorial Weighting in Game Theory	Second-Level Index	Fuzzy DEMATEL Method	Entropy Weight Method	Combinatorial Weighting in Game Theory
X_1	0.1723	0.1670	0.1686	X_{11}	0.2107	0.4848	0.4346
				X_{12}	0.2036	0.2821	0.1678
				X_{13}	0.2975	0.1598	0.2849
				X_{14}	0.2882	0.0733	0.1128
X_2	0.2418	0.1343	0.1666	X_{21}	0.1981	0.2607	0.2606
				X_{22}	0.1987	0.2768	0.2767
				X_{23}	0.2066	0.1876	0.1876
				X_{24}	0.2012	0.1621	0.1621
				X_{25}	0.1953	0.1128	0.1129
X_3	0.2329	0.1121	0.1484	X_{31}	0.1821	0.3567	0.3401
				X_{32}	0.2172	0.2416	0.2393
				X_{33}	0.1853	0.1219	0.1393
				X_{34}	0.2205	0.1453	0.1313
				X_{35}	0.1949	0.1345	0.1500
X_4	0.1517	0.3004	0.2557	X_{41}	0.3309	0.2329	0.2448
				X_{42}	0.3132	0.4616	0.4435
				X_{43}	0.3559	0.3055	0.3116
X_5	0.2014	0.2862	0.2607	X_{51}	0.2735	0.4399	0.4160
				X_{52}	0.2661	0.2871	0.2841
				X_{53}	0.2391	0.1596	0.1316
				X_{54}	0.2213	0.1135	0.1685

(2) Calculation of risk initial value

Set the initial value range between [0, 0.05]. The higher the value, the more obvious the impact on construction safety. Invite experts and scholars to score according to their experience and knowledge in combination with the construction safety status of AY Project. Finally, take the arithmetic average value as the initial value of each risk factor, as shown in Table 8.

Table 8. Initial values of risk factors.

Index	X_{11}	X_{12}	X_{13}	X_{14}	X_{21}	X_{22}	X_{23}	X_{24}	X_{25}	X_{31}	X_{32}
Initial value	0.0253	0.013	0.0116	0.0269	0.0173	0.0216	0.0136	0.0208	0.0164	0.0258	0.0275
Index	X_{33}	X_{34}	X_{35}	X_{41}	X_{42}	X_{43}	X_{51}	X_{52}	X_{53}	X_{54}	
Initial value	0.0186	0.0138	0.0177	0.0174	0.0163	0.0268	0.0166	0.0152	0.0317	0.0167	

5.3.4. Risk Simulation Analysis

The Vensim software was used to conduct the evolution analysis of safety risks in the TBM construction of hydraulic tunnels. The model time was set in months, and the system INITIALTIME was set to 0, FINALTIME to 24, and TIMESTEP to 1.

(1) Overall system safety risk evolution analysis
As shown in Figure 9, the increase in risk levels from the first month to the eighth month was relatively small. This was due to various influences such as safety education before the start of work and unfamiliarity with the construction environment, which led to a high level of vigilance among personnel. By strictly implementing safety regulations, risks related to human factors and management were effectively controlled. In addition, after the TBM was debugged and put into use for a relatively short period of time, the influence of factors such as mechanical equipment was relatively small, and no chain reaction was formed. As the construction progresses, the tunneling section passes through multiple adverse geological conditions, increasing the construction difficulty, intensifying the wear and tear of the TBM, and making the management and coordination of multi-process operations more challenging. The fatigue and complacency of personnel due to long-term work have also raised the probability of violations and operational errors. Under these associated circumstances, risks continue to evolve and accumulate. It can be seen from the evolution curve that the overall safety risk control effect of the TBM tunneling section of the AY project is generally good, which is consistent with the situation where no major safety accidents have occurred in reality, further verifying the accuracy and effectiveness of the model.

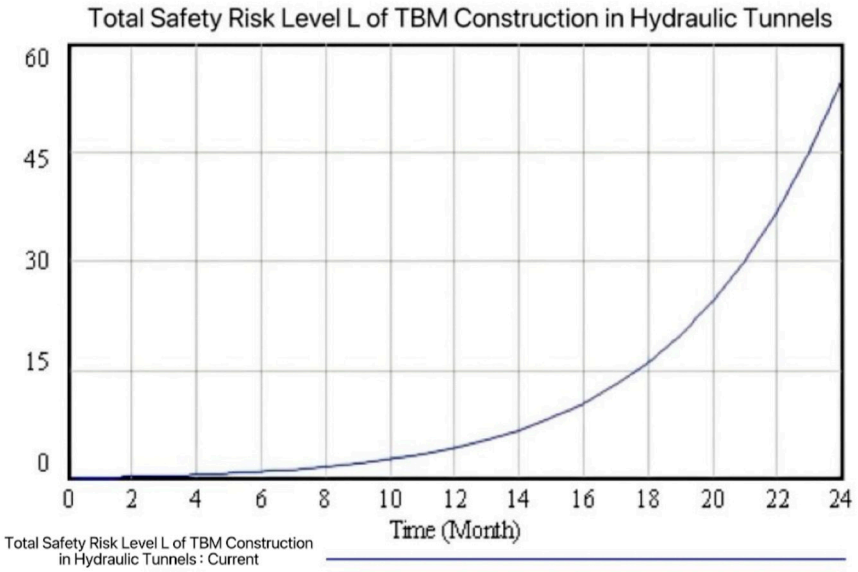


Figure 9. Evolution trend of safety risk in TBM construction of AY project.

(2) Analysis of safety risk evolution of each subsystem
The evolution trend of the security risk levels of each subsystem is shown in Figure 10. By comparing the risk level values of the vertical axes in each figure and the slope of the curve changes, the ranking of the risk levels of each subsystem from largest to smallest at the end of the simulation cycle is geology > equipment > personnel > technology > management. Overall, the changes in the risk levels of technology and management are relatively slow, and the risk levels are also low. This is in line with the situations described in the construction report regarding the resolution of construction challenges such as soil control, the continuous implementation of safety management

systems, the achievement of "zero-error" breakthrough in TBM tunneling, and the one-time qualification inspection of segment assembly quality.

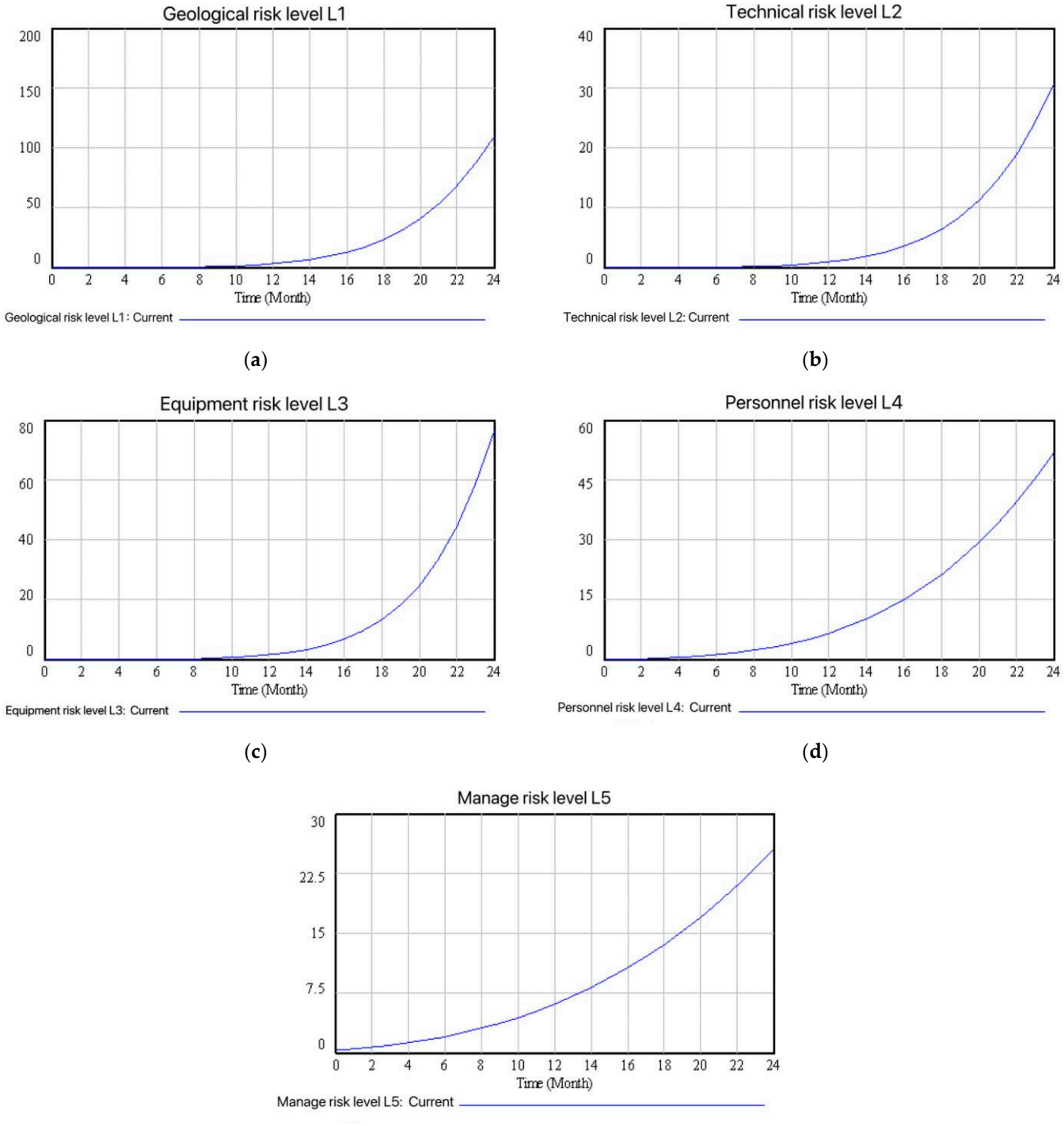


Figure 10. Evolution trend of subsystems. (**a**) Trends in geological risk evolution. (**b**) Trends in technological risk evolution. (**c**) Evolution trend of equipment risks. (**d**) Trends in personnel risk evolution. (**e**) Managing risk evolution trends.

5.3.5. Sensitivity Analysis

In order to explore more comprehensively the key subsystems and factors affecting construction safety in the associated situation, the control variable method is utilized to select two sensitivity analysis strategies: On the one hand, by adjusting the factor correlation

coefficients within each subsystem, the subsystem that is most closely associated with construction safety risks is determined; On the other hand, starting from the risk factors within a single subsystem, determine the key factors of each subsystem.

(1) Sensitivity analysis of subsystems

The correlation coefficients of the factors in the five subsystems were adjusted in sequence, and one control scheme "current" and five experimental schemes "current1–5" were set up. In the control plan, the risk correlation coefficient remains unchanged. In the experimental plan, according to the coding sequence of each subsystem, only the correlation coefficients of factors within a single subsystem are adjusted in sequence, with an adjustment range of a 50% reduction. The sensitivity comparison of each subsystem is shown in Figure 11.

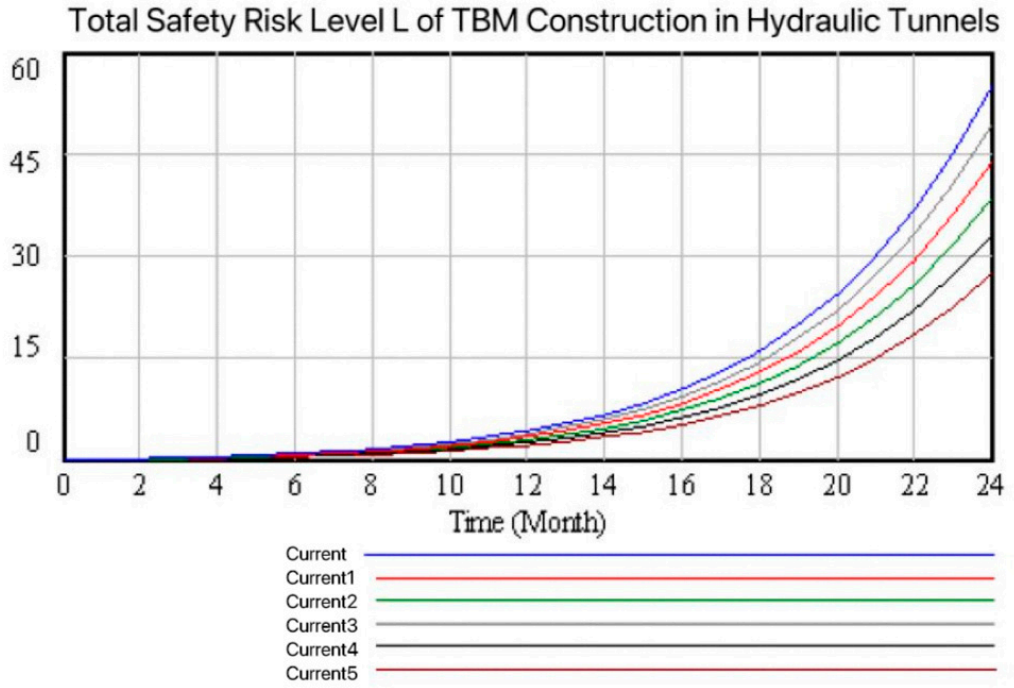


Figure 11. Comparison of sensitivity analysis of subsystem.

As can be seen from Figure 11, adjusting the degree of association in the management subsystem is the most effective in reducing the overall system security risk level, with the most obvious speed reduction. Secondly, it is personnel > technology > geology > equipment. Therefore, during construction, it is necessary to focus on reducing the transmission and correlation of management risk and personnel risk subsystem factors in the overall system.

(2) Sensitivity analysis of risk factors

Starting from the five subsystems, respectively, when analyzing the factors within one subsystem, ensure that the factor values of the other subsystems remain unchanged, and set up the control group "current" and the experimental group. Each experimental group reduced the initial risk value of a single factor by 50% in sequence according to the coding sequence of the internal factors of the subsystem. According to the above sensitivity analysis plan, the comparison of factor sensitivity analysis within each subsystem is shown in Figure 12.

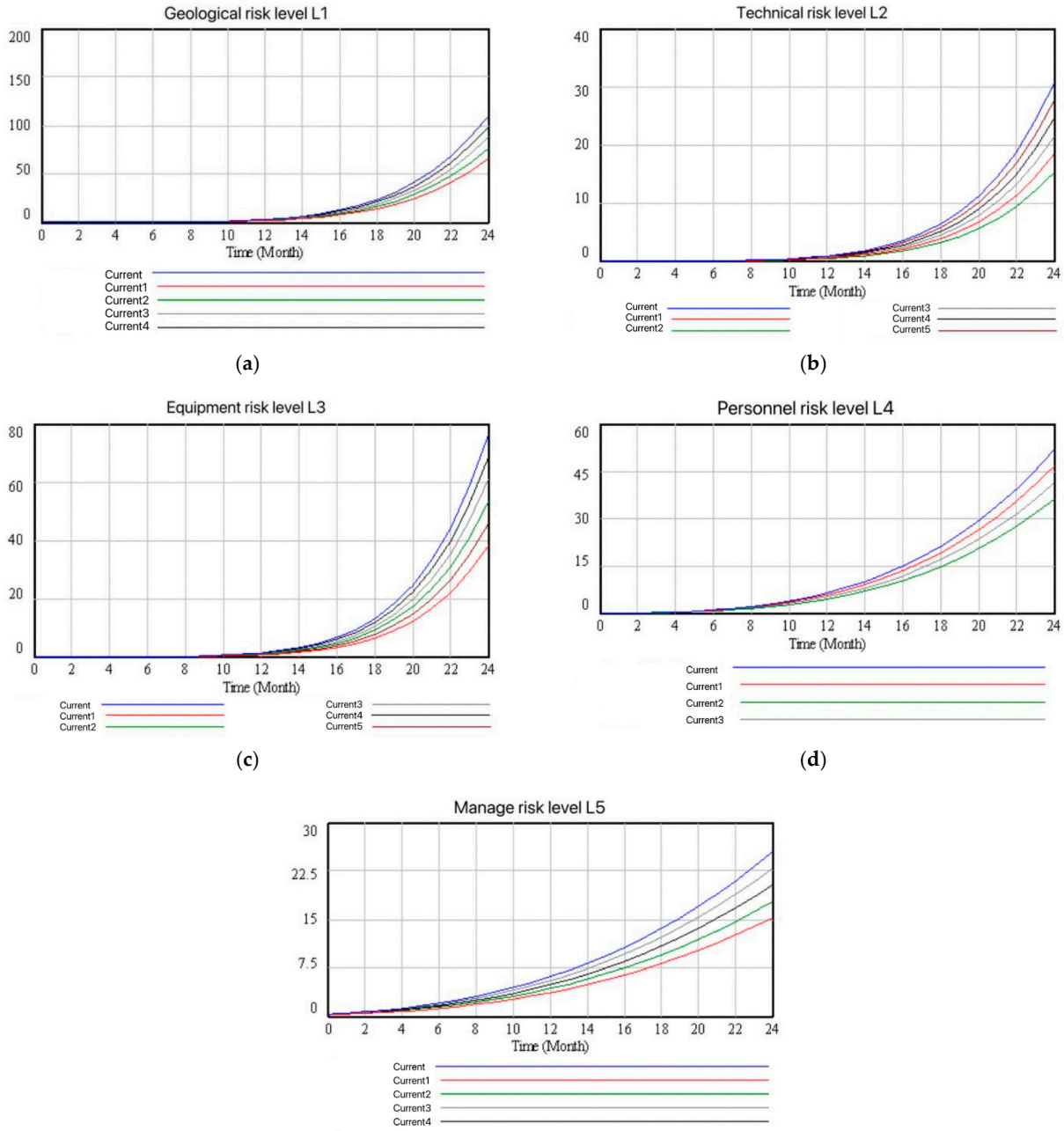


Figure 12. Comparison of sensitivity analysis of factors in each subsystem. (**a**) Geological risk subsystem. (**b**) Technical risk subsystem. (**c**) Equipment risk subsystem. (**d**) Personnel risk subsystem. (**e**) Risk management subsystem.

As can be seen from Figure 11, the most sensitive factors in each subsystem are adverse geological conditions, improper setting of construction parameters, improper equipment selection and configuration, weak safety awareness and imperfect management system. In view of the above five key risk factors, the corresponding preventive measures are proposed as follows:

(1) In response to adverse geological conditions, before construction, a comprehensive application of multi-source technical means such as ground penetrating radar and advanced drilling is carried out to conduct refined geological exploration and prediction. Meanwhile, plans for advanced grouting reinforcement and optimization of support

structures are promptly formulated to enhance the adaptability and stability of TBM tunneling in complex environments.

(2) In terms of construction parameter setting, special analysis shall be conducted on key technical parameters such as excavation mode and support technology in combination with detailed geological data, and the implementation of construction technical standards and operating procedures shall be strengthened to ensure operation in accordance with specification requirements.

(3) According to the surrounding rock grade and hydrological characteristics of different sections, TBM equipment types with strong adaptability shall be selected to avoid propulsion obstruction or efficiency reduction due to improper equipment selection.

(4) For weak safety awareness, a safety culture atmosphere shall be created, and systematic safety training shall be carried out regularly, including TBM operation procedures, risk identification, safety protection and emergency treatment knowledge, so as to prevent accidents.

(5) Establish a complete set of safety management system and operating procedures, covering all aspects of construction, clarify safety management responsibilities and emergency response procedures, and avoid problems such as management gaps or system lags.

6. Conclusions

This study aimed to systematically reveal the intrinsic correlation mechanisms and dynamic evolution patterns of safety risks in hydraulic tunnel TBM construction. By developing an integrated research framework that combines static correlation analysis with dynamic evolution simulation, the following major conclusions were drawn:

(1) A systematic risk indicator system was established. Through the collection of extensive textual data from multiple sources—including literature, engineering case reports, and interview records—and the application of grounded theory and gray relational analysis, a safety risk indicator system for hydraulic tunnel TBM construction was identified and developed. The system comprises five primary dimensions—geological, technical, equipment, personnel, and management—and 21 secondary indicators. This framework comprehensively covers the key factors influencing construction safety and provides a solid foundation for subsequent risk analysis and management.

(2) A safety risk correlation analysis model for TBM construction in hydraulic tunnels based on fuzzy DEMATEL–ISM–BN is proposed. It works as follows: Introduce fuzzy theory and use the DEMATEL method to analyze and calculate the causal attributes and importance of risk factors. Classify the risk factor levels in combination with the ISM model, and construct the risk factor association structure based on the hierarchical relationship and transmission relationship. Map the multi-layer hierarchical structure to the Bayesian network, and based on the conditional probability information, use the Euclidean distance to achieve the quantitative expression of risk association.

(3) In the case of risk correlation, the safety risk evolution of hydraulic tunnel TBM construction is studied based on system dynamics, the basic concept of system dynamics is clarified, the calculation method of model parameters and system dynamics equations are determined, and the safety risk evolution model of hydraulic tunnel TBM construction is established.

(4) Taking the AY project as an example, the validity and accuracy of the two models were verified. A risk correlation structure with a total of 7 levels was established. Further, by using the BN model, the probability of occurrence of construction safety risks in the AY project was obtained as 0.6517, and the degree of risk correlation was calculated. The simulation results of the evolution model show that the risk level

is on the rise. By adopting different sensitivity analysis strategies, it is determined that the management risk subsystem has the most significant impact on the overall risk level, and it is determined that adverse geological conditions, improper setting of construction parameters, improper equipment selection and configuration, weak safety awareness and imperfect management systems are the most sensitive factors within each subsystem. Proposing preventive measures against these key risk factors can effectively enhance the safety of engineering construction.

(5) The dynamic evolution patterns and critical subsystems of risks were revealed. The system dynamics (SD) simulation results indicated that, over the entire project cycle, the overall risk level exhibited a nonlinear upward trend. The risk levels of subsystems were ranked as follows: geological > equipment > personnel > technical > management. Further sensitivity analysis of subsystems confirmed that the management risk subsystem was the most sensitive to overall risk levels, and variations in its internal correlation strength exerted the most significant suppressive effect on global risk.

(6) Core sensitive factors within each subsystem were identified. Factor sensitivity analysis further pinpointed the most critical risk points within each subsystem, namely, "adverse geological conditions", "inappropriate construction parameter settings", "improper equipment selection and configuration", "weak safety awareness", and "inadequate management systems". Based on these identified key risk factors, targeted preventive and control measures were proposed, providing a scientific basis for improving safety management in TBM construction projects.

Author Contributions: Conceptualization, X.N.; methodology, X.N. and H.Y.; software, H.Y.; validation, X.N., J.L. and P.Z.; formal analysis, H.Y.; investigation, J.L.; resources, T.F.; data curation, H.Y.; writing—original draft preparation, H.Y.; writing—review and editing, J.L. and P.Z.; visualization, X.N.; supervision, T.F.; project administration, X.N. All authors have read and agreed to the published version of the manuscript.

Funding: This research received no external funding.

Data Availability Statement: The original contributions presented in this study are included in the article. Further inquiries can be directed to the corresponding author.

Conflicts of Interest: The authors declare no conflicts of interest.

References

1. Zhang, Z.; Wang, B.; Wang, X.; He, Y.; Wang, H.; Zhao, S. Safety-risk assessment for TBM construction of hydraulic tunnel based on fuzzy evidence reasoning. *Processes* **2022**, *10*, 2597. [CrossRef]
2. Hu, K.; Wang, J.; Wu, D.; Wang, Y. Risk Assessment of Small-Diameter Shield Construction in a Deep Drainage Tunnel Based on an ISM–CRITIC–Cloud Model. *Buildings* **2024**, *14*, 3920. [CrossRef]
3. Sharafat, A.; Latif, K.; Seo, J. Risk analysis of TBM tunneling projects based on generic bow-tie risk analysis approach in difficult ground conditions. *Tunn. Undergr. Space Technol.* **2021**, *111*, 103860. [CrossRef]
4. Chung, H.; Park, J.; Kim, B.-K.; Kwon, K.; Lee, I.-M.; Choi, H. A causal network-based risk matrix model applicable to shield TBM tunneling projects. *Sustainability* **2021**, *13*, 4846. [CrossRef]
5. Hasanpour, R.; Rostami, J.; Schmitt, J.; Ozcelik, Y.; Sohrabian, B. Prediction of TBM jamming risk in squeezing grounds using Bayesian and artificial neural networks. *J. Rock Mech. Geotech. Eng.* **2020**, *12*, 21–31. [CrossRef]
6. Wang, J.; Cheng, G.; Zhou, B.; Hu, W.; Tan, H.; Xie, J. Safety risk evaluation of long-distance small-diameter tunnel bored by tunnel boring machine. *Tunn. Constr.* **2024**, *44* (Suppl. S2), 211–223.
7. Liu, W.; Yin, H.; Su, Y.; Luo, H.; Jin, C.; Dang, D. Safety risk evaluation and diagnosis of hydraulic tunnel construction based on G2-AEW-UMT Model. *J. Water Resour. Water Eng.* **2023**, *34*, 184–192.
8. Wang, J.; Hu, D.; Wu, H.; Wang, M.; Liu, D. Risk assessment in construction of small-diameter deep drainage tunnel. *China Saf. Sci. J.* **2020**, *30*, 113–120.
9. Li, Q.; Li, Z.; Xu, L.; Wang, Y. Identification and Analysis of Risk Sources in Shield Tunneling of Diversion Tunnel. *Yellow River* **2023**, *45*, 121–125.

10. Fu, L.; Wang, X.; Zhao, H.; Li, M. Interactions among safety risks in metro deep foundation pit projects: An association rule mining-based modeling framework. *Reliab. Eng. Syst. Saf.* **2022**, *221*, 108381. [CrossRef]
11. Yan, H.; Zheng, Z.; Huang, H.; Zhou, X.; Tang, Y.; Hu, P. Risk coupling evaluation of social stability of major engineering based on N-K model. *Buildings* **2022**, *12*, 702. [CrossRef]
12. Li, F.; Wang, W.; Dubljevic, S.; Khan, F.; Xu, J.; Yi, J. Analysis on accident-causing factors of urban buried gas pipeline network by combining DEMATEL, ISM and BN methods. *J. Loss Prev. Process Ind.* **2019**, *61*, 49–57. [CrossRef]
13. Nie, X.; Zhao, T.; Zhang, P.; Fan, T.; Wang, B. Study on risk correlation analysis and risk transmission of long-distance water diversion project. *J. North China Univ. Water Resour. Electr. Power (Nat. Sci. Ed.)* **2022**, *43*, 45–53.
14. Wu, Y.; Wei, K.; Liu, Q.; Liu, F.; Li, L. Correlation Evaluation Model and Application of Construction Risk of Tunnel Freezing Method. *Chin. J. Undergr. Space Eng.* **2021**, *17*, 961–968.
15. Huang, J.W.; Fang, J.; Wang, J.C. Risk coupling analysis of metro deep foundation pit construction based on complex networks. *Buildings* **2024**, *14*, 1953. [CrossRef]
16. Wu, C.; Ou, B.; Zhao, H.; Hua, C.; Han, Z. Simulation Study on Construction Safety of Deep Foundation Pit Based on Multi-risk Coupling Effect. *Water Power* **2025**, 1–10.
17. Xie, L.; Wang, H. Research on risk evolution of cruise ship construction schedule based on SD. *China Saf. Sci. J.* **2022**, *32* (Suppl. S1), 63–71.
18. Liu, X.; Dou, Z.; Yang, W. Research on influencing factors of cross border E-commerce supply chain resilience based on integrated fuzzy DEMATEL–ISM. *IEEE Access* **2021**, *9*, 36140–36153. [CrossRef]
19. Yuan, B.; Liang, J.; Huang, X.; Huang, Q.; Zhang, B.; Yang, G.; Wang, Y.; Yuan, J.; Wang, H.; Yuan, P. Eco-efficient recycling of engineering muck for manufacturing low-carbon geopolymers assessed through LCA: Exploring the impact of synthesis conditions on performance. *Acta Geotech.* **2024**, 1–21. [CrossRef]
20. Xu, M.; Xue, Y.; Li, F.; Zhang, Y. Analysis on risk factors of coal mine gas explosion based on PSO-BP-DEMETEL model. *Saf. Coal Mines* **2022**, *53*, 164–170.
21. Xue, X.; Xin, C.; Xu, D.; Liu, T. Cause analysis of falling accidents in construction engineering based on improved ISM-MICMAC. *J. Saf. Environ.* **2023**, *23*, 2802–2809.
22. Yuan, B.; Liang, J.; Zhang, B.; Chen, W.; Huang, X.; Huang, Q.; Li, Y.; Yuan, P. Optimized reinforcement of granite residual soil via a cement and alkaline solution: A coupling effect. *J. Rock Mech. Geotech. Eng.* **2024**, *17*, 509–523. [CrossRef]
23. Yuan, B.; Huang, Q.; Xu, W.; Han, Z.; Luo, Q.; Chen, G.; Yuan, J.; Zhang, Q.; Sabri, S.M.M. Study on the interaction between pile and soil under lateral load in coral sand. *Geomech. Energy Environ.* **2025**, *42*, 100674. [CrossRef]
24. Sajid, Z.; Khan, F.; Zhang, Y. Integration of interpretive structural modelling with Bayesian network for biodiesel performance analysis. *Renew. Energy* **2017**, *107*, 194–203. [CrossRef]
25. Wares, A. Challenging problems in Euclidean geometry. *Int. J. Math. Educ. Sci. Technol.* **2020**, *51*, 626–630. [CrossRef]
26. Geng, X.; Lv, Y.; Zhao, L.; Wang, Y. Measurement and simulation of risk coupling in port hazardous chemical logistics. *Int. J. Environ. Res. Public Health* **2023**, *20*, 4008. [CrossRef] [PubMed]

Disclaimer/Publisher's Note: The statements, opinions and data contained in all publications are solely those of the individual author(s) and contributor(s) and not of MDPI and/or the editor(s). MDPI and/or the editor(s) disclaim responsibility for any injury to people or property resulting from any ideas, methods, instructions or products referred to in the content.